Supplementary Information for "Quantum Geometric Injection and Shift Optical Forces Drive Coherent Phonons"

J. Luke Pimlott[1,*] and Habib Rostami[1,†]

[1] *Department of Physics, University of Bath, Claverton Down, Bath BA2 7AY, United Kingdom*

CONTENTS

Supplementary Note 1: Kadanoff–Baym derivation of the Raman-force susceptibility 1

Supplementary Note 2: Band-basis expressions for the Raman-force diagrams 3

Supplementary Note 3: Low-output-frequency decomposition of the Raman-force response 4
A. Quantum geometry of injection contribution 5
B. Quantum geometry of shift contribution 6

Supplementary Note 4: Cancellation of counterterms between the triangle and oval diagrams 8

Supplementary Note 5: Quantum geometry of off-resonant contributions 9
A. Contribution from diagram (a): $\beta^{\mathrm{off},1}_{abc}$ 9
B. Contributions from diagram (b): $\beta^{\mathrm{off},2}_{abc}$ 9
C. Contributions from diagrams (c) and (d): $\beta^{\mathrm{off},3}_{abc}$ 10
D. Total off-resonant susceptibility and its two-band dielectric limit 10

Supplementary Note 6: Numerically-tractable form of the phononic shift vector 12

Supplementary Note 7: Length-gauge derivation of the quantum-geometric Raman force 13
A. Length-gauge injection force 15
1. Singular (conventional) injection contribution 15
2. Regular injection contribution 16
B. Length-gauge shift force 16

Supplementary Note 8: Derivation of the conventional dielectric-function limit 17

Supplementary Note 9: Symmetry constraints on Raman forces in the bilayer Haldane model 18
A. M_x: mirror covariance 18
B. C_3: rotational symmetry 19

Supplementary Note 10: Temperature dependence of linearly-polarized Raman forces 20

References 21

SUPPLEMENTARY NOTE 1: KADANOFF–BAYM DERIVATION OF THE RAMAN-FORCE SUSCEPTIBILITY

In the presence of light–matter interaction with a light field with vector potential $\mathbf{A}$ and electron-phonon interaction operator $\hat{\mathcal{M}}_a$, phonon displacement field component u_a, the thermodynamical average of the atomic force is expressed in terms of the field-dependent Green's function [1–3]

$$\mathcal{F}_a(1) = i\int_{1'}\int_{1''} \mathrm{tr}[\hat{\mathcal{M}}_a(1',1'';1)\hat{G}(1'',1')]\Big|_{\mathbf{u}\to\mathbf{0}}. \tag{S1}$$

* jlp62@bath.ac.uk
† hr745@bath.ac.uk

Here, $1 = (\mathbf{r}_1, t_1)$ is a shorthand for the space-time coordinate, $1' = 1''^{+} = (\mathbf{r}_{1''}, t_{1''} + 0^{+})$, $\mathrm{tr}[\dots]$ denotes the trace over internal spinor degrees of freedom, and the Green's function is defined as

$$\hat{G}(1,1') = -i\langle \mathcal{T}_t[\hat{\psi}_H(1)\hat{\psi}_H^{\dagger}(1')]\rangle \tag{S2}$$

in which $\langle\cdots\rangle$ stands for the thermodynamic average, $\mathcal{T}_t$ denotes the time-ordering operation, and $\hat{\psi}_H(\mathbf{r},t)$ is the field operator in the Heisenberg picture, expressed in the basis of the full Hamiltonian $\hat{\mathcal{H}}$, which includes kinetic, light–matter, and electron-phonon interaction terms. The electron-phonon coupling, $\hat{\mathcal{M}}_a$ reads

$$\hat{\mathcal{M}}_a(1',1'';1) = -\frac{\delta \hat{G}^{-1}(1',1'')}{\delta u^a(1)}\bigg|_{\mathbf{u}\to 0}, \tag{S3}$$

where the inverse Green's function obeys

$$\hat{G}^{-1}(1',1'') = \Big\{ i\partial_{t_{1'}} - \hat{H}(-i\hbar\nabla_{1'} + e\mathbf{A}(1')) - \hat{M}_a(-i\hbar\nabla_{1'} + e\mathbf{A}(1'))u^a(1') \Big\}\delta(1'-1''), \tag{S4}$$

Here, $\hat{\mathcal{H}}(\mathbf{p}) = \hat{H}(\mathbf{p}) + \hat{M}_a(\mathbf{p})u_a$ is the momentum-resolved form of Eq. (26) of the main text, while $\hat{H}(\mathbf{p}) \equiv \hat{H}(-i\hbar\nabla)$ is the noninteracting electronic Hamiltonian. The light–matter interaction is included via the minimal-coupling substitution $\mathbf{p} \to \mathbf{p} + e\mathbf{A}$, which can be expanded for small $\mathbf{A}$, giving paramagnetic (one-photon coupling) and diamagnetic (two-photon coupling) current operators, as

$$\hat{H}(\mathbf{p}) \to \hat{H}(\mathbf{p}+e\mathbf{A}) \approx \hat{H}(\mathbf{p}) + e[\nabla_{p_{b_1}}\hat{H}(\mathbf{p})]A^{b_1} + \frac{e^2}{2}[\nabla_{p_{b_1}}\nabla_{p_{b_2}}\hat{H}(\mathbf{p})]A^{b_1}A^{b_2} + \mathcal{O}(\mathbf{A}^3). \tag{S5}$$

Similarly, part of the light–matter coupling emerges as a mixed photon–phonon–electron interaction, originating from the (minimally-coupled) momentum dependence of the electron–phonon coupling, expanded to

$$\hat{M}_a(\mathbf{p}) \to \hat{M}_a(\mathbf{p}+e\mathbf{A}) \approx \hat{M}_a(\mathbf{p}) + e[\nabla_{p_{b_1}}\hat{M}_a(\mathbf{p})]A^{b_1} + \frac{e^2}{2}[\nabla_{p_{b_1}}\nabla_{p_{b_2}}\hat{M}_a(\mathbf{p})]A^{b_1}A^{b_2} + \mathcal{O}(\mathbf{A}^3), \tag{S6}$$

with repeated indices summed according to the Einstein summation convention. Following the Taylor expansion, we define the one-photon and two-photon current operators, as well as photon-phonon-electron coupling terms in the space-time coordinate basis, based on the derivatives of the inverse Green's function,

$$\nabla_{p_b}\hat{H} \quad\to\quad \hat{j}_b(1',1'';2) = \frac{\delta\hat{G}^{-1}(1',1'')}{\delta A^b(2)} \tag{S7}$$

$$\nabla_{p_b}\nabla_{p_c}\hat{H} \quad\to\quad \hat{j}_{bc}(1',1'';2,3) = \frac{\delta^2\hat{G}^{-1}(1',1'')}{\delta A^c(3)\delta A^b(2)} \tag{S8}$$

$$\nabla_{p_b}\hat{M}_a \quad\to\quad \hat{\mathcal{M}}_{ab}(1',1'';1,2) = -\frac{\delta\hat{G}^{-1}(1',1'')}{\delta A^b(2)\delta u^a(1)} \tag{S9}$$

$$\nabla_{p_b}\nabla_{p_c}\hat{M}_a \quad\to\quad \hat{\mathcal{M}}_{abc}(1',1'';1,2,3) = -\frac{\delta\hat{G}^{-1}(1',1'')}{\delta A^c(3)\delta A^b(2)\delta u^a(1)} \tag{S10}$$

(noting that $\delta G^{-1}/\delta A = -\delta\mathcal{H}/\delta A$ and $\delta G^{-1}/\delta u = -\delta\mathcal{H}/\delta u$). With the light–matter coupling term expressed in terms of the Green's function, the Raman susceptibility can be obtained by applying a variational approach and differentiating Eq. (S1) with respect to the light field:

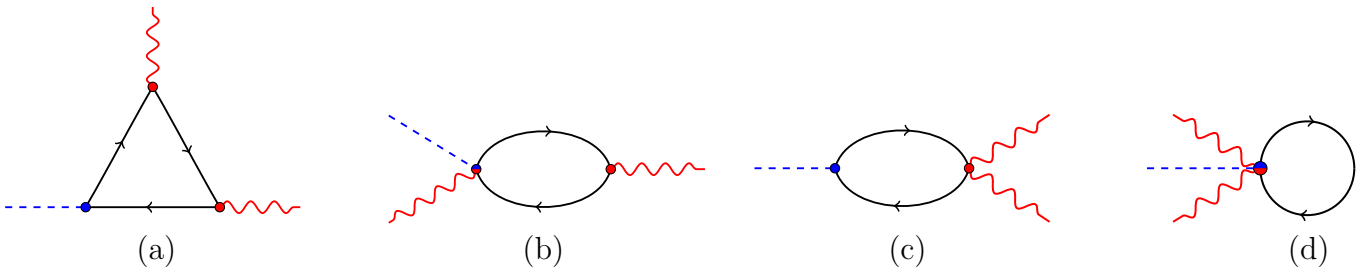
$$\pi_{abc}(1;2,3) = \frac{1}{2}\frac{\delta^2\mathcal{F}_a(1)}{\delta A_b(2)\delta A_c(3)}\bigg|_{\mathbf{A}\to\mathbf{0}}. \tag{S11}$$

The lengthy but straightforward variational calculus generates four distinct terms for the Raman response given by

$$\pi_{abc}(1;2,3) = \frac{i}{2}(\pi^{\mathrm{A}}_{abc}(1;2,3) + \pi^{\mathrm{B}}_{abc}(1;2,3) + \pi^{\mathrm{C}}_{abc}(1;2,3) + \pi^{\mathrm{D}}_{abc}(1;2,3)) \tag{S12}$$

where each term explicitly reads

$$\begin{aligned}\pi^{\mathrm{A}}_{abc}(1;2,3) = -\int_{1',1''}\int_{2',2''}\int_{3',3''}\Big\{ &\mathrm{Tr}\Big[\hat{\mathcal{M}}_a(1',1'';1)G(1'',3')\hat{j}_c(3',3'';3)G(3'',2')\hat{j}_b(2',2'';2)G(2'',1')\Big] \\ &+ \mathrm{Tr}\Big[\hat{\mathcal{M}}_a(1',1'';1)G(1'',2')\hat{j}_b(2',2'';2)G(2'',3')\hat{j}_c(3',3'';3)G(3'',1')\Big]\Big\},\end{aligned} \tag{S13}$$



Supplementary Fig. 1. The four topologically-unique Feynman diagrams for the Raman-force susceptibility: solid, dashed, and wavy lines respectively denote electrons, phonons, and photons. The diagrams from (a)–(d) respectively represent Eqs. (S13)–(S16). Diagrams (a) and (b) have two permutations.

$$\pi^{\mathrm{B}}_{abc}(1;2,3) = \int_{1',1''}\int_{2',2''}\Big\{\mathrm{Tr}\Big[\hat{\mathcal{M}}_{ab}(1',1'';1,2)G(1'',2')\hat{j}_c(2',2'';3)G(2'',1')\Big] + \mathrm{Tr}\Big[\hat{\mathcal{M}}_{ac}(1',1'';1,3)G(1'',2')\hat{j}_b(2',2'';2)G(2'',1')\Big]\Big\}, \tag{S14}$$

$$\pi^{\mathrm{C}}_{abc}(1;2,3) = \int_{1',1''}\int_{2',2''}\mathrm{Tr}\Big[\hat{\mathcal{M}}_{a}(1',1'';1)G(1'',2')\hat{j}_{bc}(2',2'';2,3)G(2'',1')\Big], \tag{S15}$$

and finally

$$\pi^{\mathrm{D}}_{abc}(1;2,3) = -\int_{1',1''}\mathrm{Tr}\Big[\hat{\mathcal{M}}_{abc}(1',1'';1,2,3)G(1'',1')\Big]. \tag{S16}$$

These terms can be illustrated using four distinct Feynman diagrams depicted in Supplementary Fig. 1. Finally, the gauge-invariant response function to the external electric fields, χ_{abc}, is obtained by relating the electric field to a homogeneous vector potential, $\mathbf{E}(t) = -\partial_t\mathbf{A}(t)$, which in the frequency domain becomes $\mathbf{A}(\omega) = \mathbf{E}(\omega)/(i\omega)$, leading to

$$\chi_{abc}(\omega_\Sigma;\omega_1,\omega_2) = \frac{\pi_{abc}(\omega_\Sigma;\omega_1,\omega_2)}{(i\omega_1)(i\omega_2)}, \tag{S17}$$

having Fourier transformed the susceptibility to the frequency domain, where our electric fields are $E^b(\omega_1)$ and $E^c(\omega_2)$, and with $\omega_\Sigma = \omega_1+\omega_2$ the frequency of the Raman force generated. Note that experimentally, one would observe both $\chi_{abc}(\omega_\Sigma;\omega_1,\omega_2)$ and $\chi_{acb}(\omega_\Sigma;\omega_2,\omega_1)$ simultaneously, which as they are equal means that the total observed response would be twice that implied by a single susceptibility component.

SUPPLEMENTARY NOTE 2: BAND-BASIS EXPRESSIONS FOR THE RAMAN-FORCE DIAGRAMS

We move from the real to imaginary-time formalism [4], allowing us to use a Matsubara summation approach in the band basis to formally evaluate each diagram in terms of electronic dispersion, and the matrix elements of light-matter and electron-phonon coupling terms. First, we fix the notation as

$$\hat{j}_{b_1b_2\ldots b_n} = -e^n\hat{v}_{b_1b_2\ldots b_n}, \qquad \hat{\mathcal{M}}_{ab_1b_2\ldots b_n} = e^n\hat{M}_{ab_1b_2\ldots b_n}, \tag{S18}$$

where $\hat{v}_b = \partial_{p_b}\hat{\mathcal{H}}$ is the velocity operator, $\hat{M}_a = \partial_{u_a}\hat{\mathcal{H}}$ is the electron-phonon coupling operator, and $\hat{M}_{ab} = \partial_{p_b}\hat{M}_a$ is the electron-phonon-photon coupling operator. In compact notation, the eigenvalue problem of the electronic Hamiltonian reads $\mathcal{H}|\phi_n\rangle = \varepsilon_n|\phi_n\rangle$, where ε_n is the energy of band n with eigenvector $|\phi_n\rangle$. The Matsubara Green's function can then be written in the band basis as

$$\langle\phi_n|\hat{G}(i\varepsilon_\nu)|\phi_m\rangle = \delta_{nm}G_n = \frac{\delta_{nm}}{i\varepsilon_\nu-\varepsilon_n}, \tag{S19}$$

where $\varepsilon_\nu = (2\nu+1)\pi k_B T$ stands for the fermionic Matsubara energy and ν is an integer. We use the standard Matsubara sums [4] for one, two and three propagators, given by

$$\frac{1}{\beta}\sum_\nu G_m(i\varepsilon_\nu) = f(\varepsilon_m) = f_m \tag{S20}$$

$$\frac{1}{\beta}\sum_\nu G_n(i\varepsilon_\nu + i\hbar\omega)G_m(i\varepsilon_\nu) = \frac{1}{\hbar}\frac{f_{mn}}{\omega+\omega_{mn}} \tag{S21}$$

$$\frac{1}{\beta}\sum_\nu G_l(i\varepsilon_\nu + i\hbar\omega)G_n(i\varepsilon_\nu + i\hbar\omega_1)G_m(i\varepsilon_\nu) = \frac{1}{\hbar^2}\left\{\frac{f_{mn}}{(\omega_1-\omega_{nm})(\omega-\omega_{lm})} + \frac{f_{ln}}{(\omega_2-\omega_{ln})(\omega-\omega_{lm})}\right\}, \tag{S22}$$

where $\beta = 1/k_B T$ is the inverse temperature and f_m denotes the Fermi–Dirac distribution for band m. We define $f_{mn} = f_m - f_n$, and $\omega_{nm} = (\varepsilon_n - \varepsilon_m)/\hbar$ is the energy difference between bands n and m, expressed in frequency units. With these sums, we compute the explicit values of each diagram, which are

$$\chi^{\mathrm{A}}_{abc}(\omega_\Sigma;\omega_1,\omega_2) = \frac{-e^2}{2\hbar^2(i\omega_1)(i\omega_2)}\sum_{\mathbf{p}}\sum_{mnl}\left\{\frac{f_{mn}M_a^{ml}v_c^{ln}v_b^{nm}}{(\omega_1+i\gamma-\omega_{nm})(\omega_\Sigma+i\Gamma-\omega_{lm})} + \frac{f_{mn}M_a^{lm}v_c^{mn}v_b^{nl}}{(\omega_2+i\gamma-\omega_{mn})(\omega_\Sigma+i\Gamma-\omega_{ml})} + [b,\omega_1\leftrightarrow c,\omega_2]\right\} \tag{S23}$$

$$\chi^{\mathrm{B}}_{abc}(\omega_\Sigma;\omega_1,\omega_2) = \frac{-e^2}{2\hbar(i\omega_1)(i\omega_2)}\sum_{\mathbf{p}}\sum_{mn}\left\{\frac{f_{mn}M_{ac}^{mn}v_b^{nm}}{\omega_1+i\gamma+\omega_{mn}} + [b,\omega_1\leftrightarrow c,\omega_2]\right\} \tag{S24}$$

$$\chi^{\mathrm{C}}_{abc}(\omega_\Sigma;\omega_1,\omega_2) = \frac{-e^2}{2\hbar(i\omega_1)(i\omega_2)}\sum_{\mathbf{p}}\sum_{mn}\frac{f_{mn}M_a^{mn}v_{bc}^{nm}}{\omega_\Sigma+i\Gamma+\omega_{mn}} \tag{S25}$$

$$\chi^{\mathrm{D}}_{abc}(\omega_\Sigma;\omega_1,\omega_2) = \frac{-e^2}{2(i\omega_1)(i\omega_2)}\sum_{\mathbf{p}}\sum_{m} f_m M_{abc}^{mm} \tag{S26}$$

where $O^{mn} = \langle\phi_m|\hat{O}|\phi_n\rangle$ is the matrix element of operator $\hat{O}$. Here, we include a small imaginary part in the frequency to account for phenomenological damping. Specifically, we add γ to the frequencies ω_1 and ω_2, and Γ to their sum, ω_Σ. Physically, in the case of rectified Raman force we are interested in, γ represents interband dephasing, while $\Gamma = \tau^{-1}$ is the intraband transport relaxation rate [5].

Unless otherwise stated, analytical expressions in the Supplementary Information are given per spin. The spin degeneracy $g_s = 2$ is included in the main-text microscopic response formulas and in all numerical results.

SUPPLEMENTARY NOTE 3: LOW-OUTPUT-FREQUENCY DECOMPOSITION OF THE RAMAN-FORCE RESPONSE

The rectified Raman-force response is obtained in the low-output-frequency regime, $\omega_\Sigma = \omega_1 + \omega_2 \to 0$, with $\omega_1 \approx -\omega_2$. In this limit, the triangle response in Eq. (S23) can be separated according to whether the EPC vertex is band diagonal, M_a^{nn}, or band off-diagonal, M_a^{mn} $(m \neq n)$. The band-diagonal EPC sector contains three contributions: the singular injection pole, proportional to $1/\omega_\Sigma$; a regular resonant correction to the injection channel; and a regular off-resonant contribution. By contrast, the band-off-diagonal EPC sector generates a counterterm, $\gamma^{\triangle}_{abc}$. We may therefore write

$$\chi^{\mathrm{A}}_{abc} = \chi^{\text{EPC-intra}}_{abc} + \chi^{\text{EPC-inter}}_{abc} = \chi^{\text{inj,sing}}_{abc} + \chi^{\text{inj,reg}}_{abc} + \chi^{\text{off,1}}_{abc} + \gamma^{\triangle}_{abc}. \tag{S27}$$

Similarly, the susceptibility in Eq. (S24) can be separated according to whether it depends on the Abelian, $\mathbb{A}_a^{nn}$, or non-Abelian, $\mathbb{A}_a^{mn}$ $(m \neq n)$, components of the Mead–Truhlar (MT) gauge connection,

$$\mathbb{A}_a^{mn} = i\,\langle\phi_m\,|\partial_{u_a}\phi_n\,\rangle_{\mathbf{u}=0}\,. \tag{S28}$$

The corresponding low-output-frequency decomposition of diagram (b) is

$$\chi^{\mathrm{B}}_{abc} = \chi^{\text{Abelian}}_{abc} + \chi^{\text{non-Abelian}}_{abc} = \chi^{\text{shi}}_{abc} + \chi^{\text{off,2}}_{abc} + \gamma^{\mathrm{O}}_{abc}. \tag{S29}$$

The Abelian sector gives the resonant shift response together with an off-resonant contribution, whereas the non-Abelian sector generates the counterterm $\gamma^{\mathrm{O}}_{abc}$, which exactly cancels $\gamma^{\triangle}_{abc}$ in the clean, noninteracting limit.

Finally, the remaining contributions from Eqs. (S25) and (S26) combine, in the low-output-frequency limit, into a single off-resonant contribution,

$$\chi^{\mathrm{C}}_{abc} + \chi^{\mathrm{D}}_{abc} = \chi^{\mathrm{off},3}_{abc}. \tag{S30}$$

Consequently, after cancellation of the counterterms, $\gamma^{\triangle}_{abc} + \gamma^{\mathrm{O}}_{abc} = 0$, as demonstrated in Supplementary Note 4, the complete low-output-frequency response separates into resonant injection and shift channels together with three off-resonant contributions. It can therefore be written as

$$\chi_{abc} \approx \chi^{\mathrm{inj,sing}}_{abc} + \chi^{\mathrm{inj,reg}}_{abc} + \chi^{\mathrm{shi}}_{abc} + \sum_{j=1}^{3} \chi^{\mathrm{off,j}}_{abc} + \mathcal{O}(\omega_\Sigma). \tag{S31}$$

The resonant injection and shift responses constitute the main focus of this work, while the complete off-resonant response is analyzed in Supplementary Note 5. In the remainder of this section, we develop the quantum-geometric decomposition of the resonant injection and shift channels, with the injection channel comprising both singular and regular contributions. We further note that the responses to linearly polarized (LP) and circularly polarized (CP) light are obtained from the corresponding symmetric and antisymmetric optical-index sectors, which reduce to the relevant real and imaginary parts of the response tensor at rectification [6].

A. Quantum geometry of injection contribution

For the band-diagonal EPC sector, $l = m$, and hence $\omega_{lm} = \omega_{ml} = 0$. Setting $\omega_1 = \omega$ and $\omega_2 = \omega_\Sigma - \omega$, and relabelling $m \leftrightarrow n$ in the appropriate terms, we obtain

$$\begin{aligned}\chi^{\mathrm{EPC-intra}}_{abc}(\omega_\Sigma;\omega,\omega_\Sigma-\omega) = &-\frac{e^2}{2\hbar^2}\frac{1}{\omega(\omega-\omega_\Sigma)}\frac{1}{\omega_\Sigma+i\Gamma}\sum_{\mathbf{p}}\sum_{mn} f_{mn}\left(M^{mm}_a - M^{nn}_a\right) v^{nm}_b v^{mn}_c \\ &\times\left[\frac{1}{\omega+i\gamma-\omega_{nm}} - \frac{1}{\omega-\omega_\Sigma-i\gamma-\omega_{nm}}\right].\end{aligned} \tag{S32}$$

The band-off-diagonal EPC sector, meanwhile, reduces in the low-output-frequency limit to

$$\begin{aligned}\lim_{\omega_\Sigma\to 0}\chi^{\mathrm{EPC-inter}}_{abc}(\omega_\Sigma;\omega,\omega_\Sigma-\omega) = \gamma^{\triangle}_{abc}(\omega) = -\frac{e^2}{2\hbar^2\omega^2}\sum_{\mathbf{p}}\sum_{mnl}\Bigg\{&\frac{f_{mn}M^{ml}_a v^{ln}_c v^{nm}_b}{(\omega+i\gamma-\omega_{nm})(i\Gamma-\omega_{lm})}\Bigg|_{l\neq m} \\ &+\frac{f_{mn}M^{lm}_a v^{mn}_c v^{nl}_b}{(-\omega+i\gamma-\omega_{mn})(i\Gamma-\omega_{ml})}\Bigg|_{l\neq m} + [b,\omega\leftrightarrow c,-\omega]\Bigg\}.\end{aligned} \tag{S33}$$

This term is exactly cancelled, in the clean noninteracting limit, by the counterterm $\gamma^{\mathrm{O}}_{abc}$ arising from diagram (b). The details of this cancellation are presented in Supplementary Note 4.

We now focus on the band-diagonal EPC sector and take the intrinsic clean limit at fixed nonzero ω_Σ, $\gamma, \Gamma \to 0^+$, consistent with the prescription used throughout the preceding sections, and only then expand for small ω_Σ. The factors entering Eq. (S32) therefore admit the expansions

$$\frac{1}{\omega(\omega-\omega_\Sigma)} = \frac{1}{\omega^2} + \frac{\omega_\Sigma}{\omega^3} + O(\omega_\Sigma^2), \tag{S34}$$

$$\frac{1}{\omega-\omega_{nm}+i0^+} - \frac{1}{\omega-\omega_{nm}-\omega_\Sigma-i0^+} = -2i\pi\delta(\omega-\omega_{nm}) - \omega_\Sigma\left[\mathcal{P}\frac{1}{(\omega-\omega_{nm})^2} - i\pi\delta'(\omega-\omega_{nm})\right] + O(\omega_\Sigma^2). \tag{S35}$$

Substituting Eqs. (S34) and (S35) into Eq. (S32), the leading terms in the ω_Σ expansion reproduce the singular injection response. Introducing the band-resolved quantum geometric tensor

$$Q^{nm}_{bc} = \frac{v^{nm}_b v^{mn}_c}{\omega^2_{nm}} = g^{nm}_{bc} - \frac{i}{2}\Omega^{nm}_{bc}, \tag{S36}$$

where g_{bc}^{nm} and Ω_{bc}^{nm} denote the band-resolved (interband) quantum metric and Berry curvature, respectively, we obtain

$$\chi_{abc}^{\mathrm{inj,sing}}(\omega_\Sigma \to 0; \omega, -\omega) = \frac{\alpha_{abc}^{\mathrm{inj}}(\omega)}{i\omega_\Sigma}, \tag{S37}$$

with

$$\alpha_{abc}^{\mathrm{inj}}(\omega) = -\frac{\pi e^2}{\hbar^2} \sum_{\mathbf{p}} \sum_{mn} f_{mn}\, \Delta_a^{mn} Q_{bc}^{nm}\, \delta(\omega - \omega_{nm}), \tag{S38}$$

where $\Delta_a^{mn} = M_a^{mm} - M_a^{nn}$. The injection susceptibility $\alpha_{abc}^{\mathrm{inj}}(\omega)$ enters the total low-output-frequency response through the singular term in Eq. (3) of the main text. Its compact quantum-geometric form closely parallels the corresponding expression for the injection photocurrent [7, 8]. The LP and CP injection responses are obtained from the real and imaginary parts of Q_{bc}^{nm}, respectively.

The remaining resonant contribution is regular in ω_Σ and arises from the $\delta(\omega - \omega_{nm})$ and $\delta'(\omega - \omega_{nm})$ terms generated by Eqs. (S34) and (S35). Their frequency dependence can be simplified using the distributional identity

$$\frac{\omega_{nm}^2}{\omega^3}\delta(\omega - \omega_{nm}) - \frac{\omega_{nm}^2}{2\omega^2}\delta'(\omega - \omega_{nm}) = -\frac{1}{2}\delta'(\omega - \omega_{nm}), \tag{S39}$$

which follows from the general distributional identity

$$f(x)\delta'(x-a) + f'(a)\delta(x-a) = f(a)\delta'(x-a). \tag{S40}$$

Using the definition of $\alpha_{abc}^{\mathrm{inj}}(\omega)$ above, the regular resonant contribution to the injection channel can therefore be written compactly as

$$\chi_{abc}^{\mathrm{inj,reg}}(\omega) \equiv \beta_{abc}^{\text{reg-inj}}(\omega) = \frac{i}{2}\frac{\partial \alpha_{abc}^{\mathrm{inj}}(\omega)}{\partial \omega}. \tag{S41}$$

Thus, the band-diagonal EPC sector of the triangle diagram contains both the singular injection pole and a regular resonant correction, with the latter entirely determined by the spectral dispersion of the injection susceptibility.

The principal-value term in Eq. (S35) gives rise to an off-resonant contribution, which is discussed separately in Supplementary Note 5.

B. Quantum geometry of shift contribution

Using the covariant derivative approach [9, 10] with respect to phonon displacement in the a-direction,

$$M_{ab}^{mn} = \langle \phi_m | \hat{M}_{ab} | \phi_n \rangle = \partial_{u_a} v_b^{mn} - i\Big[\hat{\mathbb{A}}_a, \hat{v}_b\Big]^{mn} = \partial_{u_a} v_b^{mn} - i\sum_l \left(\mathbb{A}_a^{ml} v_b^{ln} - v_b^{ml}\mathbb{A}_a^{ln}\right), \tag{S42}$$

where the Mead-Truhlar (MT) connection is defined as

$$\mathbb{A}_a^{mn} = \langle \phi_m | \hat{\mathbb{A}}_a | \phi_n \rangle = i\langle \phi_m | \partial_{u_a} | \phi_n \rangle, \tag{S43}$$

Therefore, the Abelian contribution, whose resonant component gives the shift-force susceptibility, reads

$$\lim_{\omega_\Sigma \to 0} \chi_{abc}^{\mathrm{Abelian}} = \chi_{abc}^{\mathrm{shi}}(\omega) + \chi_{abc}^{\mathrm{off,2}}(\omega) = \frac{-e^2}{2\hbar\omega^2} \sum_{\mathbf{p}} \sum_{mn} f_{mn} \left\{ \frac{\left(\partial_{u_a} v_c^{mn} - i\left(\mathbb{A}_a^{mm} v_c^{mn} - v_c^{mn}\mathbb{A}_a^{nn}\right)\right) v_b^{nm}}{\omega + i\gamma + \omega_{mn}} + [b, \omega \leftrightarrow c, -\omega] \right\}. \tag{S44}$$

and the non-Abelian counterpart, meanwhile, is given by

$$\lim_{\omega_\Sigma \to 0} \chi_{abc}^{\text{non-Abelian}} = \gamma_{abc}^{\mathrm{O}}(\omega) = \frac{-e^2}{2\hbar\omega^2} \sum_{\mathbf{p}} \sum_{mnl} f_{mn} \left\{ \frac{-i\mathbb{A}_a^{ml} v_c^{ln} v_b^{nm}\big|_{l\neq m}}{\omega + i\gamma + \omega_{mn}} + \frac{-i\mathbb{A}_a^{lm} v_c^{nl} v_b^{mn}\big|_{l\neq m}}{\omega + i\gamma - \omega_{mn}} + [b, \omega \leftrightarrow c, -\omega] \right\}, \tag{S45}$$

which cancels $\gamma^{\triangle}_{abc}(\omega)$ in the clean limit, as discussed in the following Supplementary Note 4. Turning back to the Abelian part, we represent velocity matrix elements in polar form, as $v_c^{mn} = |v_c^{mn}|e^{-i\vartheta_c^{mn}}$, which after some algebra gives us

$$\chi^{\rm shi}_{abc}(\omega) + \chi^{\rm off,2}_{abc}(\omega) = \frac{-e^2}{2\hbar\omega^2}\sum_{\mathbf{p}}\sum_{mn} f_{mn}\left\{\frac{\left(|v_b^{nm}|\partial_{u_a}|v_c^{mn}|e^{-i(\vartheta_c^{mn}+\vartheta_b^{nm})} - i\omega_{nm}^2\mathbb{R}^{mn}_{a;c}Q^{nm}_{bc}\right)}{\omega + i\gamma + \omega_{mn}} + [b,\omega\leftrightarrow c,-\omega]\right\}, \quad \text{(S46)}$$

where the *phononic shift vector*, evaluated at $\mathbf{u} = \mathbf{0}$, is defined as

$$\mathbb{R}^{mn}_{a;c} = \partial_{u_a}\vartheta_c^{mn} + \mathbb{A}_a^{mm} - \mathbb{A}_a^{nn}, \quad \text{(S47)}$$

with $\vartheta_c^{mn} = -\operatorname{Im}\ln v_c^{mn}$. This expression is invariant under independent band-dependent $U(1)$ transformations $|\phi_n\rangle \to e^{i\theta_n(\mathbf{p},\mathbf{u})}|\phi_n\rangle$. Indeed,

$$v_c^{mn} = \langle\phi_m|v_c|\phi_n\rangle \to e^{i(\theta_n-\theta_m)}v_c^{mn}, \qquad \mathbb{A}_a^{nn} = i\langle\phi_n|\partial_{u_a}\phi_n\rangle \to \mathbb{A}_a^{nn} - \partial_{u_a}\theta_n. \quad \text{(S48)}$$

Consequently,

$$\mathbb{R}^{mn}_{a;c} \to \mathbb{R}^{mn}_{a;c} - \partial_{u_a}(\theta_n-\theta_m) - \partial_{u_a}\theta_m + \partial_{u_a}\theta_n = \mathbb{R}^{mn}_{a;c}. \quad \text{(S49)}$$

Taking the resonant contribution in the clean limit, and following some basic algebra and use of the relation $v_b^{mn} = i\omega_{mn}\mathcal{A}_b^{mn}$, which expresses the interband velocity matrix element in terms of the electronic Berry connection, $\mathcal{A}_b^{mn} = i\hbar\langle\phi_m|\partial_{p_b}|\phi_n\rangle$, we obtain the shift-force susceptibility as $\beta^{\rm shi}_{abc}(\omega) \equiv \chi^{\rm shi}_{abc}(\omega)$ as

$$\beta^{\rm shi}_{abc}(\omega) = \frac{i\pi e^2}{2\hbar}\sum_{\mathbf{p}}\sum_{mn} f_{mn}\left\{\left(|\mathcal{A}_b^{nm}|\partial_{u_a}|\mathcal{A}_c^{nm}| - |\mathcal{A}_c^{nm}|\partial_{u_a}|\mathcal{A}_b^{nm}|\right)e^{-i(\vartheta_b^{nm}-\vartheta_c^{nm})} - i\left(\mathbb{R}^{mn}_{a;c}+\mathbb{R}^{mn}_{a;b}\right)Q^{nm}_{bc}\right\}\delta(\omega-\omega_{nm}). \quad \text{(S50)}$$

This expression is rather complicated and opaque, and to make progress, we consider specific cases for the response to LP and CP light separately (in the way outlined above). For LP incoming light, we can, without loss of generality, assume that the input polarizations are identical, i.e., $c = b$. In this case, the expression simplifies significantly to

$$\beta^{\rm shi-LP}_{abb}(\omega) = \frac{\pi e^2}{\hbar}\sum_{\mathbf{p}}\sum_{mn} f_{mn}\mathbb{R}^{mn}_{a;b}\operatorname{Re}\left[Q^{nm}_{bb}\right]\delta(\omega-\omega_{nm}), \quad \text{(S51)}$$

which resembles the well-known shift current formula expressed in terms of the quantum geometric tensor [7, 8], whose real part corresponds to the quantum metric.

For CP light, we reformulate the expression using the chiral Berry connection and the chiral shift vector, as introduced in the context of the gyration (circular shift) current [8]. The chiral Berry connections are defined as

$$\mathcal{A}_\pm^{mn} = \frac{1}{\sqrt{2}}(\mathcal{A}_b^{mn} \pm i\mathcal{A}_c^{mn}) = |\mathcal{A}_\pm^{mn}|e^{-i\vartheta_\pm^{mn}} = [\mathcal{A}_\mp^{nm}]^*, \quad \text{(S52)}$$

where the $\pm$ indices denote the two circular polarizations, and where ϑ_ℓ^{mn} describes the phase of both velocity and Berry connection elements beyond a constant term of $\pi/2$. The corresponding chiral phononic shift vector is given by

$$\mathbb{R}^{mn}_{a;\pm} = \partial_{u_a}\vartheta_\pm^{mn} + \mathbb{A}_a^{mm} - \mathbb{A}_a^{nn}, \quad \text{(S53)}$$

which captures the phase winding of the chiral Berry connection along with the difference in diagonal MT connections. Using these definitions, the shift-force susceptibility to CP light becomes

$$\beta^{\rm shi-CP}_{abc}(\omega) = -\frac{\pi e^2}{2\hbar}\sum_{\mathbf{p}}\sum_{mn} f_{mn}\left(|\mathcal{A}_+^{mn}|^2\mathbb{R}^{mn}_{a;+} - |\mathcal{A}_-^{mn}|^2\mathbb{R}^{mn}_{a;-}\right)\delta(\omega-\omega_{nm}). \quad \text{(S54)}$$

The squared chiral Berry amplitudes can be further expressed in terms of quantum-geometric quantities as [8]

$$|\mathcal{A}_\pm^{mn}|^2 = \frac{g_{bb}^{mn} + g_{cc}^{mn} \mp \Omega_{bc}^{mn}}{2}. \quad \text{(S55)}$$

Substituting this back into the previous expression yields

$$\beta^{\mathrm{shi-CP}}_{abc}(\omega) = -\frac{\pi e^2}{4\hbar}\sum_{\mathbf{p}}\sum_{mn} f_{mn}\left\{(g^{mn}_{bb}+g^{mn}_{cc})(\mathbb{R}^{mn}_{a;+}-\mathbb{R}^{mn}_{a;-}) - \Omega^{mn}_{bc}(\mathbb{R}^{mn}_{a;+}+\mathbb{R}^{mn}_{a;-})\right\}\delta(\omega-\omega_{nm}), \tag{S56}$$

where we see contributions from both the symmetric (quantum metric) and antisymmetric (Berry curvature) parts of the quantum geometric tensor. This structure highlights the geometric origin of the Raman-force response under circularly polarized excitation, which closely resembles that of the nonlinear photocurrent reported in Ref. [8].

The off-resonant contribution $\chi^{\mathrm{off},2}_{abc}(\omega)$ originates from the principal-value term in Eq. (S46) and is discussed in Supplementary Note 5.

SUPPLEMENTARY NOTE 4: CANCELLATION OF COUNTERTERMS BETWEEN THE TRIANGLE AND OVAL DIAGRAMS

In the contributions from the injection and shift diagrams (Supplementary Fig. 1a,b), after removing the parts that contribute to the injection and shift-force susceptibilities, we are left with:

$$\gamma^{\triangle}_{abc}(\omega)+\gamma^{\mathrm{O}}_{abc}(\omega) = \frac{-e^2}{2\hbar^2\omega^2}\sum_{\mathbf{p}}\sum_{mnl} f_{mn}\Bigg\{\frac{M^{ml}_a v^{ln}_c v^{nm}_b\big|_{l\neq m}}{(\omega+i\gamma-\omega_{nm})(i\Gamma-\omega_{lm})} + \frac{M^{lm}_a v^{mn}_c v^{nl}_b\big|_{l\neq m}}{(-\omega+i\gamma-\omega_{mn})(i\Gamma-\omega_{ml})}$$
$$+\frac{-i\hbar\mathbb{A}^{ml}_a v^{ln}_c v^{nm}_b\big|_{l\neq m}}{\omega+i\gamma+\omega_{mn}} + \frac{-i\hbar\mathbb{A}^{lm}_a v^{nl}_c v^{mn}_b\big|_{l\neq m})}{\omega+i\gamma-\omega_{mn}} + [b,\omega\leftrightarrow c,-\omega]\Bigg\}. \tag{S57}$$

We treat the response in the intrinsic geometric limit, where impurity, disorder, and many-body scattering (dephasing) rates are negligible. The intrinsic response is obtained by first taking the clean limit, $\lim_{\{\Gamma,\gamma\}\to 0^+}$, at fixed band gap, and for the gapless case, the gap is sent to zero at the end: $\lim_{\mathrm{gap}\to 0}\lim_{\{\Gamma,\gamma\}\to 0^+}$. This protocol captures the clean-system cancellation of the first and second lines in the above expression, independent of the magnitude of the band gap—that is, it remains valid even for an infinitesimal gap, as long as the gap exceeds the negligible scattering rates. Therefore, in this limit, we can neglect the Γ term and replace $i\Gamma-\omega_{lm}\to-\omega_{lm}$ in the denominators on the first line, yielding:

$$\gamma^{\triangle}_{abc}(\omega)+\gamma^{\mathrm{O}}_{abc}(\omega) = \frac{-e^2}{2\hbar^2\omega^2}\sum_{\mathbf{p}}\sum_{mnl} f_{mn}\Bigg\{\frac{M^{ml}_a v^{ln}_c v^{nm}_b\big|_{l\neq m}}{(\omega+i\gamma+\omega_{mn})(\omega_{ml})} + \frac{M^{lm}_a v^{mn}_c v^{nl}_b\big|_{l\neq m}}{(-\omega+i\gamma-\omega_{mn})(\omega_{lm})}$$
$$+\frac{-i\hbar\mathbb{A}^{ml}_a v^{ln}_c v^{nm}_b\big|_{l\neq m}}{\omega+i\gamma+\omega_{mn}} + \frac{-i\hbar\mathbb{A}^{lm}_a v^{nl}_c v^{mn}_b\big|_{l\neq m}}{\omega+i\gamma-\omega_{mn}} + [b,\omega\leftrightarrow c,-\omega]\Bigg\}. \tag{S58}$$

Now, using the identity $M^{ml}_a = i\hbar\omega_{ml}\mathbb{A}^{ml}_a$ for $m\neq l$ in the second line, and then simplifying and explicitly showing all terms, we get

$$\gamma^{\triangle}_{abc}(\omega)+\gamma^{\mathrm{O}}_{abc}(\omega) = \frac{e^2}{2\hbar^2\omega^2}\sum_{\mathbf{p}}\sum_{mnl}\frac{f_{mn}}{\omega_{lm}}\Bigg\{\frac{M^{ml}_a v^{ln}_c v^{nm}_b}{\omega+i\gamma+\omega_{mn}} - \frac{M^{lm}_a v^{mn}_b v^{nl}_c}{\omega+i\gamma-\omega_{mn}} + \frac{M^{ml}_a v^{ln}_b v^{nm}_c}{-\omega+i\gamma+\omega_{mn}} - \frac{M^{lm}_a v^{mn}_c v^{nl}_b}{-\omega+i\gamma-\omega_{mn}}$$
$$-\frac{M^{ml}_a v^{ln}_c v^{nm}_b}{\omega+i\gamma+\omega_{mn}} + \frac{M^{lm}_a v^{nl}_c v^{mn}_b}{\omega+i\gamma-\omega_{mn}} - \frac{M^{ml}_a v^{ln}_b v^{nm}_c}{-\omega+i\gamma+\omega_{mn}} + \frac{M^{lm}_a v^{nl}_b v^{mn}_c}{-\omega+i\gamma-\omega_{mn}}\Bigg\}\Bigg|_{l\neq m}, \tag{S59}$$

and thus in the clean limit we obtain an identically exact cancellation:

$$\gamma^{\triangle}_{abc}(\omega)+\gamma^{\mathrm{O}}_{abc}(\omega) = 0, \tag{S60}$$

as the terms on the top row clearly each cancel with the term directly below it. This reasoning can be compared to the cancellation of the counter terms for the injection and shift photocurrents, following a similar logic to that used in Sec. III D of Ref. [8], for example.

SUPPLEMENTARY NOTE 5: QUANTUM GEOMETRY OF OFF-RESONANT CONTRIBUTIONS

Here we examine the complete off-resonant Raman-force response, which consists of three distinct contributions. The first, $\beta^{\mathrm{off},1}_{abc}$, originates from the band-diagonal EPC sector of the triangle diagram in Eq. (S23), represented by Supplementary Fig. 1a, and arises from the principal-value part of its low-output-frequency expansion. The second, $\beta^{\mathrm{off},2}_{abc}$, comes from the Abelian sector of Eq. (S24), represented by Supplementary Fig. 1b, which also generates the resonant shift force. The third, $\beta^{\mathrm{off},3}_{abc}$, is obtained from the remaining susceptibilities in Eqs. (S25) and (S26), represented by the diagrams in Supplementary Fig. 1c and d. Together,

$$\beta^{\mathrm{off}}_{abc} = \beta^{\mathrm{off},1}_{abc} + \beta^{\mathrm{off},2}_{abc} + \beta^{\mathrm{off},3}_{abc}. \tag{S61}$$

These contributions are regular in the low-output-frequency limit and are dispersive rather than on shell, being governed by principal-value terms rather than the Dirac delta functions associated with the resonant injection and shift responses. Except for the nonlinear Drude term contained in $\beta^{\mathrm{off},3}_{abc}$, they can be expressed in terms of the quantum geometric tensor, closely paralleling the geometric structure of the resonant response.

A. Contribution from diagram (a): $\beta^{\mathrm{off},1}_{abc}$

We begin with the off-resonant contribution from the triangle diagram in Supplementary Fig. 1a, whose band-diagonal EPC sector also generates the resonant injection response. At leading order, taking the principal-value part of the clean-limit in the singular injection term gives

$$\alpha^{\mathrm{off}}_{abc}(\omega) = -\frac{e^2}{2\hbar^2\omega^2}\sum_{\mathbf{p}}\sum_{mn} f_{mn}\,\mathcal{P}\left\{\frac{(M^{mm}_a - M^{nn}_a)\,\omega^2_{nm}Q^{nm}_{bc}}{\omega-\omega_{nm}} - \frac{(M^{mm}_a - M^{nn}_a)\,\omega^2_{nm}Q^{nm}_{bc}}{\omega-\omega_{nm}}\right\} = 0. \tag{S62}$$

Thus, the leading principal-value counterpart of the singular injection pole cancels identically. This cancellation, however, does not exclude a regular off-resonant contribution arising at the next order in the low-output-frequency expansion. Indeed, the principal-value term in Eq. (S35), which arises from the same band-diagonal EPC sector responsible for the regular injection response, gives

$$\beta^{\mathrm{off},1}_{abc}(\omega) = \frac{e^2}{2\hbar^2}\sum_{\mathbf{p}}\sum_{mn} f_{mn}\,\Delta^{mn}_a Q^{nm}_{bc}\left(\frac{\omega_{nm}}{\omega}\right)^2 \mathcal{P}\frac{1}{(\omega-\omega_{nm})^2}. \tag{S63}$$

Eq. (S63) is a regular impulsive contribution arising from the same band-diagonal EPC sector of the triangle diagram that generates the singular and regular resonant injection responses. Unlike those resonant contributions, however, $\beta^{\mathrm{off},1}_{abc}$ belongs to the off-resonant sector that is governed by a principal-value double pole.

B. Contributions from diagram (b): $\beta^{\mathrm{off},2}_{abc}$

Next, we consider the off-resonant component of the oval diagram in Supplementary Fig. 1b, which serves as the off-resonant analogue to the shift force. Taking the principal value part of the clean limit of Eq. (S44) yields

$$\beta^{\mathrm{off},2}_{abc}(\omega) = \frac{-e^2}{2\hbar\omega^2}\sum_{\mathbf{p}}\sum_{mn} f_{mn}\mathcal{P}\left\{\frac{v^{nm}_b\partial_{u_a}v^{mn}_c - i\big(\mathbb{A}^{mm}_a - \mathbb{A}^{nn}_a\big)v^{nm}_b v^{mn}_c}{\omega-\omega_{nm}} + [b,\omega\leftrightarrow c,-\omega]\right\}. \tag{S64}$$

Writing explicitly the second term and exchanging $m \leftrightarrow n$ in this term yields, after some algebra, an expression in terms of the quantum geometric tensor Q^{nm}_{bc}:

$$\beta^{\mathrm{off},2}_{abc}(\omega) = \frac{-e^2}{2\hbar^2\omega^2}\sum_{\mathbf{p}}\sum_{mn} f_{mn}\mathcal{P}\left\{\frac{2\omega_{nm}\Delta^{nm}_a Q^{nm}_{bc} + \hbar\omega^2_{nm}\partial_{u_a}Q^{nm}_{bc}}{\omega-\omega_{nm}}\right\}, \tag{S65}$$

where we use that EPC-difference, $\Delta^{nm}_a = \hbar\partial_{u_a}\omega_{nm}$. In the second term, it enters via a displacement derivative, $\partial_{u_a}Q^{mn}_{bc}$: the phononic counterpart to the momentum-derivatives of Q^{mn}_{bc} that define quantum-geometric *dipole moments* in the photogalvanic effect [8, 11]. For LP and CP responses, we respectively call these the phononic dipole moments of quantum metric and Berry curvature.

C. Contributions from diagrams (c) and (d): $\beta^{\text{off},3}_{abc}$

Here we analyze the remaining diagrams in Supplementary Fig. 1c, d, corresponding to the terms given in Eqs. (S25) and (S26), which contribute to the susceptibility as

$$\chi^{\text{C}}_{abc}(\omega)+\chi^{\text{D}}_{abc}(\omega)=\frac{-e^2}{2\omega^2}\sum_{\mathbf{p}}\left\{\sum_m f_m M^{mm}_{a;bc}+\sum_{mn}\frac{f_{mn}M^{mn}_a v^{nm}_{bc}}{i\hbar\Gamma-\varepsilon_{nm}}\right\}. \tag{S66}$$

Using the covariant derivative from Eq. (S42) in the first term, expressing $M^{mn}_a = i\varepsilon_{mn}\mathbb{A}^{mn}_a$ and following some algebra, we rewrite the expression as

$$\chi^{\text{C}}_{abc}(\omega)+\chi^{\text{D}}_{abc}(\omega)=\frac{-e^2}{2\omega^2}\sum_{\mathbf{p}}\left\{\sum_m f_m\partial_{u_a}v^{mm}_{bc}+\sum_{mn}f_{mn}\left[\frac{M^{mn}_a v^{nm}_{bc}}{\varepsilon_{nm}}+\frac{M^{mn}_a v^{nm}_{bc}}{i\hbar\Gamma-\varepsilon_{nm}}\right]\right\}. \tag{S67}$$

Assuming a clean system far from band-touching (so that $i\hbar\Gamma$ can be neglected), the last two terms cancel, leaving

$$\beta^{\text{off},3}_{abc}(\omega)=\chi^{\text{C}}_{abc}(\omega)+\chi^{\text{D}}_{abc}(\omega)=\frac{-e^2}{2\omega^2}\sum_{\mathbf{p}}\sum_m f_m\partial_{u_a}v^{mm}_{bc}. \tag{S68}$$

Expanding this using the symmetrized (in p_b and p_c) momentum covariant derivative [9], and substituting $\partial_{u_a}v^{mm}_b = \partial_{p_b}M^{mm}_a$ and $v^{mn}_c = -i\omega_{nm}\mathcal{A}^{mn}_c$, we obtain

$$\beta^{\text{off},3}_{abc}(\omega)=\frac{-e^2}{2\omega^2}\sum_{\mathbf{p}}\left\{\sum_m f_m\partial_{p_b}\partial_{p_c}M^{mm}_a+\frac{1}{2\hbar}\sum_{mn}f_{mn}\partial_{u_a}\left(\frac{v^{mn}_b v^{nm}_c+v^{mn}_c v^{nm}_b}{\omega_{nm}}\right)\right\}. \tag{S69}$$

In the first term, the p-derivatives can be moved onto f_m, while the quantum metric appears in the second, giving

$$\beta^{\text{off},3}_{abc}(\omega)=\frac{-e^2}{2\omega^2}\sum_{\mathbf{p}}\left\{\sum_m\left(\partial_{p_b}\partial_{p_c}f_m\right)M^{mm}_a-\frac{1}{\hbar}\sum_{mn}f_{mn}\left(\frac{\Delta^{mn}_a}{\hbar}g^{mn}_{bc}+\omega_{mn}\partial_{u_a}g^{mn}_{bc}\right)\right\}. \tag{S70}$$

The first term resembles a higher-order Drude response, which describes the Drude DC photocurrent if the electron-phonon coupling operator is replaced by the velocity operator (i.e., $\hat{M}_a \to \hat{v}_a$), and shows the usual divergence for $\omega \to 0$ [8]. The second term, meanwhile, includes the phononic dipole moment of the quantum metric, similar to that in Eq. (S65). Since this expression is fully real, it contributes only to the response under LP light.

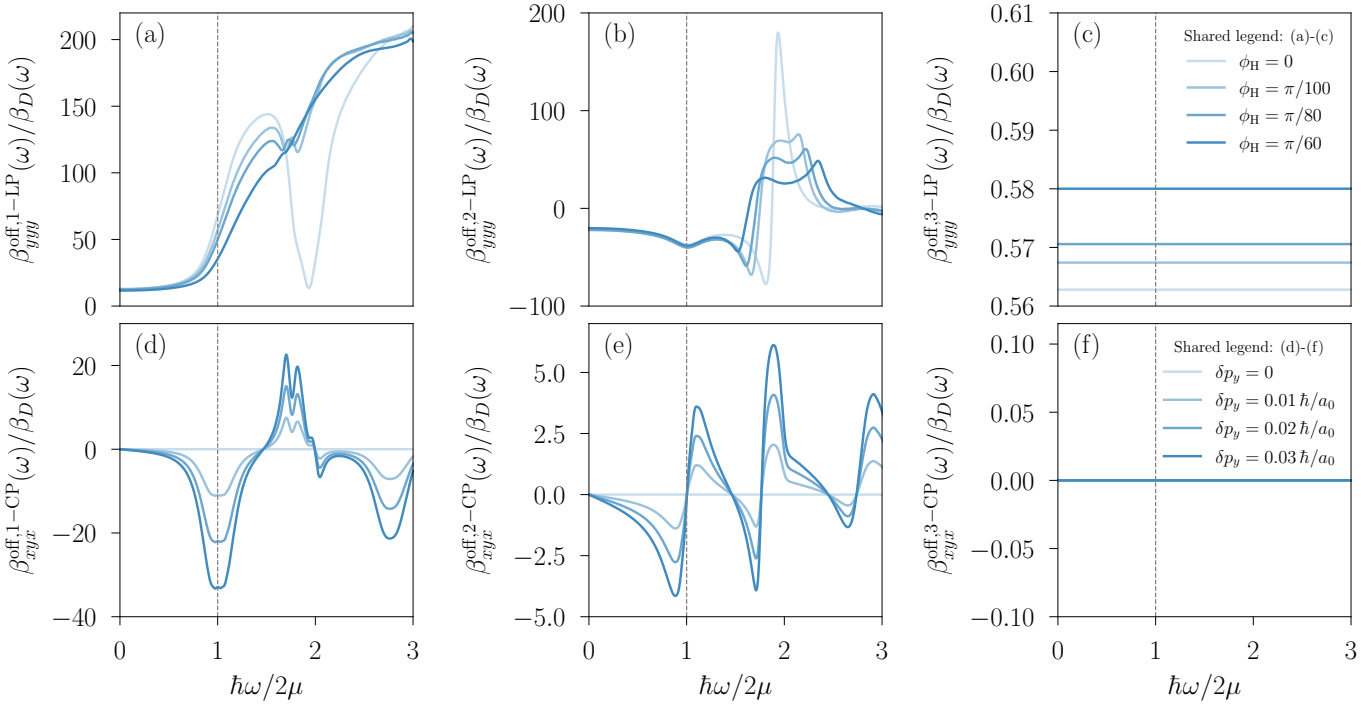
Supplementary Fig. 2 shows the LP (a–c) and CP (d–f) components of the three off-resonant contributions in the bilayer Haldane model. The responses are normalized to remove the common ω^{-2} prefactor. The first two contributions, $\beta^{\text{off},1}_{abc}$ and $\beta^{\text{off},2}_{abc}$, exhibit interband features at the same transition energies as the resonant responses, but with distinct spectral profiles. The third contribution, $\beta^{\text{off},3}_{abc}$, scales as ω^{-2} in the LP channel, giving the frequency-independent normalized curves in panel (c). Its CP component vanishes identically [panel (f)], as predicted by Eq. (S70), even in the presence of Haldane and sublattice gaps and a current-induced momentum shift that breaks C_3 symmetry.

D. Total off-resonant susceptibility and its two-band dielectric limit

Here, we reorganize the principal-value terms of the first two off-resonant contributions obtained above into a form that can be directly compared with the length-gauge result. This is achieved using exact partial-fraction decompositions of the frequency-dependent kernels. In particular,

$$\frac{\omega_{nm}}{\omega^2}\mathcal{P}\left(\frac{1}{\omega-\omega_{nm}}\right)=-\frac{1}{\omega^2}-\frac{1}{\omega_{nm}\omega}+\frac{1}{\omega_{nm}}\mathcal{P}\left(\frac{1}{\omega-\omega_{nm}}\right), \tag{S71}$$

$$\frac{\omega^2_{nm}}{\omega^2}\mathcal{P}\left(\frac{1}{(\omega-\omega_{nm})^2}\right)=\frac{1}{\omega^2}+\frac{2}{\omega_{nm}\omega}-\frac{2}{\omega_{nm}}\mathcal{P}\left(\frac{1}{\omega-\omega_{nm}}\right)+\mathcal{P}\left(\frac{1}{(\omega-\omega_{nm})^2}\right). \tag{S72}$$



Supplementary Fig. 2. Spectra of the LP components (a–c) and CP components (d–f) of $\beta^{\mathrm{off},1}_{abc}(\omega)$ [Eq. (S63)], $\beta^{\mathrm{off},2}_{abc}(\omega)$ [Eq. (S65)], and $\beta^{\mathrm{off},3}_{abc}(\omega)$ [Eq. (S70)], respectively, in the bilayer Haldane model. Each response is scaled by the frequency-dependent factor $\beta_D(\omega) = (\mu/\hbar\omega)^2\,\mathrm{nN/V^2}$. The LP components (a–c) are obtained by varying the Haldane phase ϕ_H with no sublattice gap, $\delta = 0$, whereas the CP components (d–f) are obtained by varying δp_y, the electronic momentum shift induced by a source–drain current along the y direction, with $\delta = 0.05\,\mathrm{eV}$. In panel (f), the result remains zero even when finite values of $\phi_H = \pi/80$ and $\delta p_x = 0.03\,\hbar/a_0$ are introduced to further enhance symmetry breaking. The model parameters are listed in Fig. 4 of the main text.

Substituting these in, we can rewrite the first two off-resonant susceptibilities as

$$\beta^{\mathrm{off},1}_{abc}(\omega) = \frac{e^2}{2\hbar^2}\sum_{\mathbf{p}}\sum_{mn} f_{mn}\,\Delta^{mn}_a Q^{nm}_{bc}\left\{\frac{1}{\omega^2} + \frac{2}{\omega_{nm}\omega} - \frac{2}{\omega_{nm}}\mathcal{P}\left(\frac{1}{\omega-\omega_{nm}}\right) + \mathcal{P}\left(\frac{1}{(\omega-\omega_{nm})^2}\right)\right\} \tag{S73}$$

$$\beta^{\mathrm{off},2}_{abc}(\omega) = \frac{e^2}{2\hbar^2}\sum_{\mathbf{p}}\sum_{mn} f_{mn}(2\Delta^{mn}_a Q^{nm}_{bc} - \hbar\omega_{nm}\partial_{u_a} Q^{nm}_{bc})\left\{-\frac{1}{\omega^2} - \frac{1}{\omega_{nm}\omega} + \frac{1}{\omega_{nm}}\mathcal{P}\left(\frac{1}{\omega-\omega_{nm}}\right)\right\}. \tag{S74}$$

Adding these together, we see that many Δ^{mn}_a-dependent terms will cancel, leaving

$$\beta^{\mathrm{off},1+2}_{abc}(\omega) = \frac{e^2}{2\hbar^2}\sum_{\mathbf{p}}\sum_{mn} f_{mn}\left[\mathcal{P}\left(\frac{\Delta^{mn}_a Q^{nm}_{bc}}{(\omega-\omega_{nm})^2}\right) - \mathcal{P}\left(\frac{\hbar\partial_{u_a} Q^{nm}_{bc}}{\omega-\omega_{nm}}\right) + \frac{\hbar\partial_{u_a} Q^{nm}_{bc}}{\omega} - \frac{\Delta^{mn}_a Q^{nm}_{bc}}{\omega^2} + \frac{\hbar\omega_{nm}\partial_{u_a} Q^{nm}_{bc}}{\omega^2}\right]. \tag{S75}$$

One can prove that the third term is purely Berry-curvature dependent and that the last two terms are purely quantum-metric dependent by splitting them in half and swapping m and n indices in one of the halves. Adding the third off-resonant contribution, $\beta^{\mathrm{off},3}_{abc}(\omega)$ from Eq. (S70), then gives the total off-resonant Raman susceptibility:

$$\beta^{\mathrm{off}}_{abc}(\omega) = \frac{e^2}{2}\sum_{\mathbf{p}}\sum_{mn}\left[\frac{1}{\hbar^2}\mathcal{P}\left(\frac{f_{mn}\Delta^{mn}_a Q^{nm}_{bc}}{(\omega-\omega_{nm})^2}\right) - \frac{1}{\hbar}\mathcal{P}\left(\frac{f_{mn}\partial_{u_a} Q^{nm}_{bc}}{\omega-\omega_{nm}}\right) - \frac{i f_{mn}\partial_{u_a}\Omega^{nm}_{bc}}{2\hbar\omega} - \frac{\delta_{nm}(\partial_{p_b}\partial_{p_c} f_m) M^{mm}_a}{\omega^2}\right], \tag{S76}$$

giving us squared and normal principal value contributions, a phononic Berry curvature dipole term and the nonlinear Drude contribution as the four off-resonant terms, just as one obtains from the length gauge [8].

Upon taking the two-band insulator with no Fermi surface, and where the EPC operator only contains momentum-independent intraband terms, which is the system we take when obtaining the conventional dielectric limit for the Raman force tensor in Supplementary Note 8, only the first term from above will contribute. The final term vanishes as derivatives of the Fermi-Dirac function vanish.

For the second and third term, their vanishing is apparent from the length-gauge derivation of Supplementary Note 7, as these terms come from the second and third term of Eq. (S99), which require non-zero interband EPC elements. One can also check this by using Eq. (S110) to rewrite the phononic quantum geometric dipole moment within our approximated system as

$$\partial_{u_a} Q_{bc}^{nm} = \hbar \left(\mathcal{A}_c^{mn} \partial_b \mathbb{A}_a^{nm} + \mathcal{A}_b^{nm} \partial_c \mathbb{A}_a^{mn} \right), \tag{S77}$$

which when substituting back into the relevant terms of $\beta_{abc}^{\text{off}}(\omega)$ gives zero for $n = m$ terms due to f_{mn} and also gives zero for $m \neq n$ due to the identity $\mathbb{A}_a^{nm} = -iM_a^{nm}/\varepsilon_{nm}$, with $M_a^{nm} = M_a^{mm}\delta_{nm}$. Therefore, in this approximated case, the off-resonant response is reduced to

$$\beta_{abc}^{\text{off}}(\omega) \approx -\frac{e^2\Delta_a^{cv}}{2\hbar^2} \sum_{\mathbf{p}} \mathcal{P}\left(\frac{Q_{bc}^{cv}}{(\omega-\omega_{cv})^2} + \frac{Q_{bc}^{vc}}{(\omega+\omega_{cv})^2} \right) = \frac{e^2\Delta_a^{cv}}{2\hbar^2} \sum_{\mathbf{p}} \frac{\mathrm{d}}{\mathrm{d}\omega} \mathcal{P}\left(\frac{Q_{bc}^{cv}}{\omega-\omega_{cv}} + \frac{Q_{bc}^{vc}}{\omega+\omega_{cv}} \right), \tag{S78}$$

where the ω-derivative form is what is used to obtain the dielectric-limit expression for the Raman force susceptibility. With $c = b$, one can finally reduce further to

$$\beta_{abb}^{\text{off}}(\omega) \approx \frac{e^2\Delta_a^{cv}}{2\hbar^2} \sum_{\mathbf{p}} \frac{\mathrm{d}}{\mathrm{d}\omega} \mathcal{P}\left(\frac{2\omega \mathcal{A}_b^{vc}\mathcal{A}_b^{cv}}{\omega^2-\omega_{cv}^2} \right) = \frac{e^2\Delta_a^{cv}}{2\hbar^2} \sum_{\mathbf{p}} \frac{\mathrm{d}}{\mathrm{d}\omega} \mathcal{P}\left(\frac{\omega}{\omega_{cv}} \frac{2\omega_{cv}\mathcal{A}_b^{vc}\mathcal{A}_b^{cv}}{\omega^2-\omega_{cv}^2} \right), \tag{S79}$$

using $Q_{bb}^{cv} = Q_{bb}^{vc} = \mathcal{A}_b^{vc}\mathcal{A}_b^{cv}$, which contains exactly the derivative of ω/ω_{cv} multiplied to the principal value part of linear electric susceptibility, $\chi_{bb}^{(1)}(\omega)$ of Eq. (S117). Therefore, the off-resonant part of the dielectric-limit Raman-force susceptibility evaluated in Supplementary Note 8 from the length-gauge results is consistent with our velocity-gauge results, along with the resonant term. The resulting expressions in terms of the dielectric tensor, ϵ_{bb} of Eq. (S121) and main text Eq. (20) therefore follow directly from the velocity-gauge results.

SUPPLEMENTARY NOTE 6: NUMERICALLY-TRACTABLE FORM OF THE PHONONIC SHIFT VECTOR

Here, we discuss how we obtain the phononic shift vector given by Eq. (S47) in our numerical computation. It is difficult to evaluate directly due to the derivative with respect to phonon displacement, so we find an alternative form. We note that this method is easily transferable to compute the usual shift vector describing the shift photocurrent. We start with the numerically-accessible term $M_{ab}^{mn}v_b^{nm}$, which upon expansion with the phononic covariant derivative of Eq. (S42) gives us, after use of the polar form for v_b^{nm} and some algebra, that

$$\begin{aligned} M_{ab}^{mn}v_b^{nm} =& (\partial_{u_a}|v_b^{mn}|)|v_b^{nm}|e^{-i(\vartheta_b^{mn}+\vartheta_b^{nm})} - i(\partial_{u_a}\vartheta_b^{mn})v_b^{mn}v_b^{nm} - iv_b^{mn}v_b^{nm}(\mathbb{A}_a^{mm}-\mathbb{A}_a^{nn}) \\ & -i\sum_l \left\{ \mathbb{A}_a^{ml}v_b^{ln}\Big|_{l\neq m} - \mathbb{A}_a^{ln}v_b^{ml}\Big|_{l\neq n} \right\} v_b^{nm}, \end{aligned} \tag{S80}$$

where the phases (which are antisymmetric in n and m) cancel in the first term, and we see the phononic shift vector as defined in Eq. (S47) appear between the second and third terms. Hence, we have

$$M_{ab}^{mn}v_b^{nm} = |v_b^{nm}|\partial_{u_a}|v_b^{mn}| - i|v_b^{mn}|^2\mathbb{R}_{a;b}^{mn} - i\sum_l \left\{ \mathbb{A}_a^{ml}v_b^{ln}\Big|_{l\neq m} - \mathbb{A}_a^{ln}v_b^{ml}\Big|_{l\neq n} \right\} v_b^{nm}. \tag{S81}$$

As the first term is fully real, the second is fully imaginary, while the third is, in general, complex, we can take just the imaginary part of both sides to get

$$\mathrm{Im}(M_{ab}^{mn}v_b^{nm}) = -|v_b^{mn}|^2\mathbb{R}_{a;b}^{mn} - \mathrm{Im}\left\{ i\sum_l (\mathbb{A}_a^{ml}v_b^{ln}\Big|_{l\neq m} - \mathbb{A}_a^{ln}v_b^{ml}\Big|_{l\neq n})v_b^{nm} \right\}. \tag{S82}$$

In the second term on the right-hand side, we can use $M_a^{mn} = i\varepsilon_{mn}\mathbb{A}_a^{mn}$ for $m \neq n$ to eliminate the non-Abelian MT connection. Then, by simple rearrangement, we finally obtain the shift vector as

$$\mathbb{R}_{a;b}^{mn} = -\frac{\mathrm{Im}(M_{ab}^{mn}v_b^{nm}) + \mathrm{Im}\sum_l \left\{ \frac{M_a^{ml}v_b^{ln}v_b^{nm}}{\varepsilon_{ml}}\Big|_{l\neq m} - \frac{M_a^{ln}v_b^{ml}v_b^{nm}}{\varepsilon_{ln}}\Big|_{l\neq n} \right\}}{|v_b^{mn}|^2}, \tag{S83}$$

which is easily calculable numerically. We can perform similar analysis to obtain the chiral phononic shift vector of Eq. (S53) in a numerically accessible form, which leads to

$$\mathbb{R}^{mn}_{a;\pm} = -\frac{\mathrm{Im}(M^{mn}_{a;\pm}v^{nm}_{\mp}) + \mathrm{Im}\sum_l \left\{ \frac{M^{ml}_a v^{ln}_{\pm} v^{nm}_{\mp}}{\varepsilon_{ml}}\Big|_{l\neq m} - \frac{M^{ln}_a v^{ml}_{\pm} v^{nm}_{\mp}}{\varepsilon_{ln}}\Big|_{l\neq n} \right\}}{\left|v^{mn}_{\pm}\right|^2}. \tag{S84}$$

Both the linear and chiral phononic shift vector expressions can be simplified further by canceling a factor of v^{nm}_b and $v^{nm}_{\mp}$, respectively. The two can then be written in a unified form, given by

$$\mathbb{R}^{mn}_{a;\ell} = -\,\mathrm{Im}\left\{ \frac{M^{mn}_{a\ell}}{v^{mn}_{\ell}} + \sum_{l\neq m} \frac{M^{ml}_a v^{ln}_{\ell}}{\varepsilon_{ml} v^{mn}_{\ell}} - \sum_{l\neq n} \frac{M^{ln}_a v^{ml}_{\ell}}{\varepsilon_{ln} v^{mn}_{\ell}} \right\}, \tag{S85}$$

with $\ell \to b$ for the linear and $\ell \to \pm$ for the chiral case. This expression can be simplified for the low-energy two-band system which we use later in the main text, where sums over bands l each give only one term, and where $\hat{M}_a$ has no p-dependence. In this case, we get

$$\mathbb{R}^{mn,\text{2-band}}_{a;\ell} = \mathrm{Im}\left\{ \frac{M^{mn}_a (v^{mm}_{\ell} - v^{nn}_{\ell})}{\varepsilon_{mn} v^{mn}_{\ell}} \right\}. \tag{S86}$$

SUPPLEMENTARY NOTE 7: LENGTH-GAUGE DERIVATION OF THE QUANTUM-GEOMETRIC RAMAN FORCE

To begin, we write the length-gauge many-body Hamiltonian in terms of fermionic field operators:

$$\hat{H}(t) = \int d^d\mathbf{r}\, \hat{\Psi}^\dagger(\mathbf{r}) \left[\hat{H}_e + e\,\mathbf{E}(t)\cdot\mathbf{r} \right] \hat{\Psi}(\mathbf{r}), \tag{S87}$$

where $\hat{\Psi}(\mathbf{r})$ is the fermionic field operator, $\hat{h}_e$ is the single-particle electronic Hamiltonian, and $e > 0$, such that the electronic charge is $-e$. The term $e\,\mathbf{E}(t)\cdot\mathbf{r}$ is the electric-dipole light–matter interaction in the length gauge. Expanding the field operator in Bloch eigenstates,

$$\hat{\Psi}(\mathbf{r}) = \sum_{n,\mathbf{p}} \phi_{n\mathbf{p}}(\mathbf{r})\, \hat{c}_{n\mathbf{p}}, \qquad \phi_{n\mathbf{p}}(\mathbf{r}) = \langle \mathbf{r}|\phi_{n\mathbf{p}}\rangle = e^{i\mathbf{p}\cdot\mathbf{r}/\hbar} u_{n\mathbf{p}}(\mathbf{r}), \tag{S88}$$

the Hamiltonian in the band basis becomes

$$\hat{H}(t) = \sum_{n,\mathbf{p}} \varepsilon_n(\mathbf{p}) \hat{c}^\dagger_{n\mathbf{p}} \hat{c}_{n\mathbf{p}} + e\,\mathbf{E}(t)\cdot \sum_{nm} \sum_{\mathbf{p},\mathbf{p}'} \hat{c}^\dagger_{n\mathbf{p}} \langle \phi_{n\mathbf{p}}|\hat{\mathbf{r}}|\phi_{m\mathbf{p}'}\rangle\, \hat{c}_{m\mathbf{p}'}. \tag{S89}$$

Here, $\varepsilon_n(\mathbf{p})$ is an eigenvalue of the field-free electronic Hamiltonian $\hat{H}_e$, with the corresponding Bloch eigenstate $|\phi_{n\mathbf{p}}\rangle$ satisfying

$$\hat{H}_e\,|\phi_{n\mathbf{p}}\rangle = \varepsilon_n(\mathbf{p})\,|\phi_{n\mathbf{p}}\rangle\,. \tag{S90}$$

The index n labels electronic band, while $\mathbf{p}$ denotes the crystal momentum. The position operator is not diagonal in crystal momentum and must be treated through its full momentum-space kernel [12]

$$\langle \phi_{n\mathbf{p}}|\hat{\mathbf{r}}|\phi_{m\mathbf{p}'}\rangle = i\hbar\,\delta_{nm}\,\nabla_{\mathbf{p}}\delta(\mathbf{p}-\mathbf{p}') + \boldsymbol{\mathcal{A}}_{nm}(\mathbf{p})\,\delta(\mathbf{p}-\mathbf{p}'), \tag{S91}$$

where

$$\mathcal{A}^{nm}_a(\mathbf{p}) = i\hbar\,\langle u_{n\mathbf{p}}|\partial_{p_a} u_{m\mathbf{p}}\rangle\,. \tag{S92}$$

is the non-Abelian Berry connection component in the band basis. It is useful to consider the action of the position operator on an arbitrary state $|\phi_f\rangle$, projected onto the Bloch state $|\phi_n, \mathbf{p}\rangle$:

$$\begin{aligned}\langle\phi_{n\mathbf{p}}|\hat{\mathbf{r}}|\phi_f\rangle &= \sum_{m,\mathbf{p}'}\langle\phi_{n\mathbf{p}}|\hat{\mathbf{r}}|\phi_{m\mathbf{p}'}\rangle\langle\phi_{m\mathbf{p}'}|\phi_f\rangle \\ &= \sum_{m,\mathbf{p}'}\left[i\hbar\,\delta_{nm}\nabla_{\mathbf{p}}\delta(\mathbf{p}-\mathbf{p}') + \boldsymbol{\mathcal{A}}_{nm}(\mathbf{p})\delta(\mathbf{p}-\mathbf{p}')\right]\langle\phi_{m\mathbf{p}'}|\phi_f\rangle \\ &= i\hbar\,\nabla_{\mathbf{p}}\langle\phi_{n\mathbf{p}}|\phi_f\rangle + \sum_m \boldsymbol{\mathcal{A}}_{nm}(\mathbf{p})\langle\phi_{m\mathbf{p}}|\phi_f\rangle \\ &= \sum_m\left[i\hbar\,\delta_{nm}\nabla_{\mathbf{p}} + \boldsymbol{\mathcal{A}}_{nm}(\mathbf{p})\right]\langle\phi_{m\mathbf{p}}|\phi_f\rangle. \end{aligned} \tag{S93}$$

Therefore, one may use the following notation for the band-basis momentum-diagonal notation for the position operator components [8, 13]:

$$\mathbf{r}_{nm}(\mathbf{p}) \equiv i\hbar\delta_{nm}\nabla_{\mathbf{p}} + \boldsymbol{\mathcal{A}}_{nm}(\mathbf{p}). \tag{S94}$$

We now give the derivation of the injection and shift RF susceptibilities in the length gauge, following a similar process to [8]. The atomic force is the electronic expectation value of the EPC operator, which can be written as a trace over the reduced density matrix (RDM), $\hat{\rho}(t)$, as

$$\mathbf{F}(t) = -\left\langle\frac{\partial H}{\partial\mathbf{u}}\right\rangle = -\operatorname{Tr}\left[\hat{\mathbf{M}}\hat{\rho}(t)\right] = -\sum_{\mathbf{p}}\sum_{nm}\mathbf{M}_{mn}(\mathbf{p})\rho_{nm}(\mathbf{p},t), \tag{S95}$$

which is similar in meaning to Eq. (S1) (written in terms of the RDM instead of Green's functions), and where the time-dependence of the RDM is determined by the Liouville equation:

$$i\hbar\frac{\partial\rho_{nm}(\mathbf{p},t)}{\partial t} = \left[\hat{H}(\mathbf{p},t),\hat{\rho}(\mathbf{p},t)\right]_{nm}. \tag{S96}$$

The time-dependence comes exclusively from the incident electric fields, $\mathbf{E}(t)$, and the Hamiltonian excludes the electron-phonon coupling term, as this would result in $\mathbf{F}\sim\mathcal{O}\left(\hat{\mathbf{M}}^2\right)$, leaving only the electronic and dipole components. By splitting the two remaining components of the Hamiltonian, rearranging and Fourier transforming, we obtain the recursive equation for the RDM,

$$(\omega-\omega_{nm})\,\rho^{(i+1)}_{nm}(\mathbf{p},\omega) = \frac{e}{\hbar}\int\frac{\mathrm{d}\omega_i}{2\pi}E_b(\omega-\omega_i)\left\langle\phi_{n\mathbf{p}}\middle|\left[\hat{r}_b,\hat{\rho}^{(i)}(\omega_i)\right]\middle|\phi_{m\mathbf{p}}\right\rangle, \tag{S97}$$

where $\hat{\rho}^{(i)}(\omega_i)$ is the RDM term which is to the ith order in $\mathbf{E}$, where ω_i is the total of all i electric field frequencies, and using the Blount position operator notation [13] defined in Eq. (S94). We solve Eq. (S97) iteratively to obtain increasing orders of the RDM, using the zero-order term $\rho^{(0)}_{nm}(\mathbf{p},\omega) = 2\pi\delta(\omega)f_n(\mathbf{p})\delta_{nm}$ as our starting point. Following two iterations, and symmetrizing the result for the two electric fields, we obtain the second-order RDM term as

$$\begin{aligned}\rho^{(2)}_{nm}(\mathbf{p},\omega_\Sigma) = \frac{e^2}{2\hbar^2}\int\frac{\mathrm{d}\omega_1}{2\pi}\Bigg[\Bigg(&\frac{(i\hbar)^2(\partial_c\partial_b f_m)\delta_{nm}}{(\omega_\Sigma+i\Gamma)(\omega_1+i\gamma)} \\ &+\frac{i\hbar(\partial_b f_{mn})\mathcal{A}^{nm}_c}{(\omega_\Sigma+i\Gamma-\omega_{nm})(\omega_1+i\gamma)} \\ &+\frac{i\hbar}{\omega_\Sigma+i\Gamma-\omega_{nm}}\partial_c\left(\frac{f_{mn}\mathcal{A}^{nm}_b}{\omega_1+i\gamma-\omega_{nm}}\right) \\ &+\sum_l\frac{1}{\omega_\Sigma+i\Gamma-\omega_{nm}}\left[\frac{f_{ml}\mathcal{A}^{nl}_c\mathcal{A}^{lm}_b}{\omega_1+i\gamma-\omega_{lm}} - \frac{f_{ln}\mathcal{A}^{nl}_b\mathcal{A}^{lm}_c}{\omega_1+i\gamma-\omega_{nl}}\right]\Bigg) \\ &\times E_b(\omega_1)E_c(\omega_2) + [b,\omega_1\leftrightarrow c,\omega_2]\Bigg], \end{aligned} \tag{S98}$$

with $\omega_\Sigma = \omega_1 + \omega_2$, and including the small imaginary components γ and Γ as we did before. Substituting this into Eq. (S95), we obtain the full expression for the susceptibility of the Raman force: the EPC-induced atomic force second-order in $\mathbf{E}$, as

$$\begin{aligned}\chi_{abc}(\omega_1,\omega_2) = -\frac{e^2}{2\hbar^2}\sum_{\mathbf{p}}\Bigg[&\sum_m \frac{(i\hbar)^2 M_a^{mm}(\partial_c\partial_b f_m)}{(\omega_\Sigma + i\Gamma)(\omega_1+i\gamma)} \\ &+\sum_{mn}\frac{i\hbar(\partial_b f_{mn})M_a^{mn}\mathcal{A}_c^{nm}}{(\omega_\Sigma+i\Gamma-\omega_{nm})(\omega_1+i\gamma)} \\ &+\sum_{mn}\frac{i\hbar M_a^{mn}}{\omega_\Sigma+i\Gamma-\omega_{nm}}\partial_c\left(\frac{f_{mn}\mathcal{A}_b^{nm}}{\omega_1+i\gamma-\omega_{nm}}\right) \\ &-\sum_{mnl}\left[\frac{f_{mn}M_a^{nl}\mathcal{A}_c^{lm}\mathcal{A}_b^{mn}}{(\omega_\Sigma+i\Gamma-\omega_{ln})(\omega_1+i\gamma-\omega_{mn})} - \frac{f_{mn}M_a^{lm}\mathcal{A}_b^{mn}\mathcal{A}_c^{nl}}{(\omega_\Sigma+i\Gamma-\omega_{ml})(\omega_1+i\gamma-\omega_{mn})}\right] \\ &+[b,\omega_1\leftrightarrow c,\omega_2]\Bigg]. \end{aligned} \tag{S99}$$

Here, we consider only the third and fourth contributions from above, which give the resonant interband contributions in the clean limit of $\gamma,\Gamma\to 0$, leading to the injection and shift responses in the rectified case of $\omega_\Sigma\to 0$.

A. Length-gauge injection force

First, we consider the fourth and final term, taking $\omega_1=\omega$ and $\omega_2=\omega_\Sigma-\omega$, with rectification corresponding to $\omega_\Sigma\to 0$, and keep only the terms in the sum with diagonal elements of $\tilde{M}_a$ (which we denote with superscript d), which leads to

$$\chi_{abc}^{(\mathrm{IV;d})}(\omega,\omega_\Sigma-\omega) = \frac{e^2}{2\hbar^2}\lim_{\omega_\Sigma\to 0}\frac{1}{\omega_\Sigma+i\Gamma}\sum_{\mathbf{p}}\sum_{mn}\left[\frac{f_{mn}\Delta_a^{nm}\mathcal{A}_c^{nm}\mathcal{A}_b^{mn}}{\omega+i\gamma-\omega_{mn}} + \frac{f_{mn}\Delta_a^{nm}\mathcal{A}_b^{nm}\mathcal{A}_c^{mn}}{\omega_\Sigma-\omega+i\gamma-\omega_{mn}}\right], \tag{S100}$$

with $\Delta_a^{mn} = M_a^{mm} - M_a^{nn}$. We discuss the remaining off-diagonal portion later. As in the velocity gauge, we Taylor expand the second fraction in small ω_Σ:

$$\lim_{\Gamma\to 0}\frac{1}{\omega_\Sigma+i\Gamma}\frac{1}{\omega_\Sigma-\omega+i\gamma-\omega_{nm}} \approx \lim_{\Gamma\to 0}\frac{1}{\omega_\Sigma+i\Gamma}\frac{1}{-\omega+i\gamma-\omega_{nm}} - \lim_{\Gamma\to 0}\frac{\omega_\Sigma}{\omega_\Sigma+i\Gamma}\frac{1}{(-\omega+i\gamma-\omega_{nm})^2} + \mathcal{O}(\omega_\Sigma). \tag{S101}$$

In the rectification limit, the zeroth- and first-order terms yield the singular and regular contributions, respectively, which we now consider in turn

1. *Singular (conventional) injection contribution*

The zeroth-order term in the expansion of Eq. (S101) gives

$$\chi_{abc}^{(\mathrm{IV;d;0})}(\omega) = \frac{e^2}{2\hbar^2}\lim_{\omega_\Sigma\to 0}\lim_{\Gamma\to 0}\frac{1}{\omega_\Sigma+i\Gamma}\sum_{\mathbf{p}}\sum_{mn}\left[\frac{f_{mn}\Delta_a^{nm}\mathcal{A}_c^{nm}\mathcal{A}_b^{mn}}{\omega+i\gamma-\omega_{mn}} + \frac{f_{mn}\Delta_a^{nm}\mathcal{A}_b^{nm}\mathcal{A}_c^{mn}}{-\omega+i\gamma-\omega_{mn}}\right], \tag{S102}$$

We first take the clean limit $\gamma,\Gamma\to 0^+$ at fixed nonzero ω_Σ, and only then take the rectification limit $\omega_\Sigma\to 0$. Using $1/(x+i0^+) = \mathcal{P}(1/x) - i\pi\delta(x)$ and exchanging the band labels $m\leftrightarrow n$ in one of the two terms, the principal-value contributions cancel, whereas the resonant delta-function contributions add. This yields

$$\chi_{abc}^{(\mathrm{IV;d;0})}(\omega) = \frac{-i\pi e^2}{\hbar^2}\lim_{\omega_\Sigma\to 0}\frac{1}{\omega_\Sigma}\sum_{\mathbf{p}}\sum_{mn} f_{mn}\Delta_a^{nm}\mathcal{A}_c^{mn}\mathcal{A}_b^{nm}\delta(\omega-\omega_{nm}). \tag{S103}$$

Multiplying by $i\omega_\Sigma$ before taking the rectification limit $\omega_\Sigma\to 0$, and using the band-resolved quantum geometric tensor $Q_{bc}^{nm} = \mathcal{A}_b^{nm}\mathcal{A}_c^{mn}$, we obtain

$$\alpha_{abc}^{\mathrm{inj}}(\omega) = \frac{\pi e^2}{\hbar^2}\sum_{\mathbf{p}}\sum_{mn} f_{mn}\Delta_a^{nm}Q_{bc}^{nm}\delta(\omega-\omega_{nm}). \tag{S104}$$

Equivalently,

$$\chi^{\mathrm{IV;d}}_{abc}(\omega) = \lim_{\omega_\Sigma \to 0} \frac{\alpha^{\mathrm{inj}}_{abc}(\omega)}{i\omega_\Sigma}. \tag{S105}$$

This is the exact resonant displacive susceptibility describing the injection Raman force in the length gauge. Its linearly and circularly polarized components are given in Eqs. (7) and (12) of the main text, respectively.

2. *Regular injection contribution*

The first-order term in the expansion of Eq. (S101) gives the regular injection contribution,

$$\chi^{(\mathrm{IV;d;1})}_{abc}(\omega) = \frac{e^2}{2\hbar^2} \lim_{\omega_\Sigma \to 0} \frac{\omega_\Sigma}{\omega_\Sigma + i\Gamma} \sum_{\mathbf{p}} \sum_{mn} \partial_\omega \left[\frac{f_{mn} \Delta^{nm}_a \mathcal{A}^{nm}_b \mathcal{A}^{mn}_c}{\omega - i\gamma - \omega_{nm}} \right]. \tag{S106}$$

As above, we first take the clean limit $\gamma, \Gamma \to 0^+$ at fixed nonzero ω_Σ, followed by the rectification limit $\omega_\Sigma \to 0$. Retaining the resonant delta-function contribution and introducing the band-resolved quantum geometric tensor then gives

$$\chi^{(\mathrm{IV;d;1})}_{abc}(\omega) = \frac{i\pi e^2}{2\hbar^2} \sum_{\mathbf{p}} \sum_{mn} \partial_\omega \Big[f_{mn} \Delta^{nm}_a Q^{nm}_{bc} \delta(\omega - \omega_{nm}) \Big]. \tag{S107}$$

Using the definition of the injection susceptibility, this can be written as

$$\beta^{\mathrm{reg-inj}}_{abc}(\omega) = \chi^{(\mathrm{IV;d;1})}_{abc}(\omega) = \frac{i}{2} \partial_\omega \alpha^{\mathrm{inj}}_{abc}(\omega), \tag{S108}$$

in agreement with the corresponding velocity-gauge result.

B. Length-gauge shift force

We now consider the third term in the full expression for χ_{abc}. In the rectification limit $\omega_\Sigma \to 0$, we integrate by parts to move the momentum derivative, use the off-diagonal ($m \neq n$) identity $M^{mn}_a = i\hbar\omega_{mn}\mathbb{A}^a_{mn}$ (the diagonal sector does not contribute, since $f_{mn} = 0$ for $m = n$), and then take $\Gamma \to 0$. This leaves

$$\chi^{(\mathrm{III})}_{abc}(\omega) = -\frac{e^2}{2} \sum_{\mathbf{p}} \sum_{mn} \left[\frac{f_{mn} \mathcal{A}^{nm}_b (\partial_c \mathbb{A}^{mn}_a)}{\omega + i\gamma - \omega_{nm}} + \frac{f_{mn} \mathcal{A}^{nm}_c (\partial_b \mathbb{A}^{mn}_a)}{-\omega + i\gamma - \omega_{nm}} \right]. \tag{S109}$$

From here, we substitute

$$\hbar \partial_b \mathbb{A}^{mn}_a = \partial_{u_a} \mathcal{A}^{mn}_b + i\mathcal{A}^{mn}_b (\mathbb{A}^{nn}_a - \mathbb{A}^{mm}_a) + \sum_l \left(\frac{\mathcal{A}^{ml}_b M^{ln}_a}{\hbar\omega_{ln}} \Big|_{l \neq n} - \frac{M^{ml}_a \mathcal{A}^{ln}_b}{\hbar\omega_{ml}} \Big|_{l \neq m} \right), \tag{S110}$$

which can be derived by expanding $\mathbb{A}^{mn}_a$ in Dirac notation, using the product rule to act ∂_b on this and also to move ∂_{u_a}. Keeping only the first two terms of this substituting expression, we obtain the effective diagonal (d) portion of this susceptibility term, given by

$$\chi^{(\mathrm{III;d})}_{abc}(\omega) = -\frac{e^2}{2\hbar} \sum_{\mathbf{p}} \sum_{mn} \left[\frac{f_{mn} \mathcal{A}^{nm}_b (\partial_{u_a} \mathcal{A}^{mn}_c + i\mathcal{A}^{mn}_c (\mathbb{A}^{nn}_a - \mathbb{A}^{mm}_a))}{\omega + i\gamma - \omega_{nm}} + \frac{f_{mn} \mathcal{A}^{nm}_c (\partial_{u_a} \mathcal{A}^{mn}_b + i\mathcal{A}^{mn}_b (\mathbb{A}^{nn}_a - \mathbb{A}^{mm}_a))}{-\omega + i\gamma - \omega_{nm}} \right], \tag{S111}$$

with the remaining off-diagonal portion canceling with the off-diagonal term from $\chi^{(\mathrm{IV})}_{abc}$ in exactly the way shown in Supplementary Note 4 for the velocity gauge derivation. Turning back to the diagonal component, the resonant (delta function-containing) contribution from taking the clean limit is

$$\chi^{(\mathrm{III;d},\delta)}_{abc}(\omega) = \frac{i\pi e^2}{2\hbar} \sum_{\mathbf{p}} \sum_{mn} f_{mn} \Big(\big(|\mathcal{A}^{nm}_b| \partial_{u_a} |\mathcal{A}^{mn}_c| - |\mathcal{A}^{mn}_c| \partial_{u_a} |\mathcal{A}^{nm}_b| \big) e^{-i(\vartheta^{nm}_b - \vartheta^{nm}_c)} - i \left(\mathbb{R}^{mn}_{a;c} + \mathbb{R}^{mn}_{a;b} \right) Q^{nm}_{bc} \Big) \delta(\omega - \omega_{nm}), \tag{S112}$$

upon writing in terms of the quantum geometric tensor and using the definition of the phononic shift vector, $\mathbb{R}^{mn}_{a;c}$, of Eq. (S47) and Eq. (10) of the main text (and where the Berry connections in polar form are $\mathcal{A}^{nm}_b = |\mathcal{A}^{nm}_b| e^{-i\vartheta^{nm}_b}$). Comparing with Eq. (S50), we identify the expression above as the resonant impulsive shift-force susceptibility,

$$\chi^{(\mathrm{III;d},\delta)}_{abc}(\omega) = \beta^{\mathrm{shi}}_{abc}(\omega). \tag{S113}$$

Considering this, one can follow the exact derivation of the "Shift force" subsection of Supplementary Note 3 to obtain the linear and circular shift responses described respectively by Eqs. (7) and (13) of the main text.

Thus, we conclude that both the shift and injection-force susceptibilities are obtained consistently within the length-gauge formulation.

SUPPLEMENTARY NOTE 8: DERIVATION OF THE CONVENTIONAL DIELECTRIC-FUNCTION LIMIT

Here, we take our expression for the Raman-force susceptibility derived in the length gauge and apply the approximations and assumptions from Ref. [14], which they use to be able to write in terms of the dielectric tensor. First, we assume that there is no Fermi surface and that we are at zero temperature (so that derivatives of f_n vanish), and that only intraband matrix elements of the EPC tensor exist ($M^{nm}_a = M^{nn}_a \delta_{mn}$). In this scenario, Eq. (S99) is heavily simplified to

$$\chi_{abc} \approx \frac{e^2}{2\hbar^2} \frac{1}{\omega_\Sigma + i\Gamma} \sum_{\mathbf{p}} \sum_{mn} \left(\frac{f_{mn}(M^{nn}_a - M^{mm}_a)\mathcal{A}^{mn}_b \mathcal{A}^{nm}_c}{\omega_1 + i\gamma - \omega_{mn}} + \frac{f_{mn}(M^{nn}_a - M^{mm}_a)\mathcal{A}^{mn}_b \mathcal{A}^{nm}_c}{\omega_2 + i\gamma - \omega_{nm}} \right). \tag{S114}$$

We now make a further approximation, taking a two-band insulator model with one valence band, v and conduction band c, with $f_v = 1$ and $f_c = 0$, and that $M^{cc}_a - M^{vv}_a = \overline{\Delta}_a$, which we take as momentum-independent. In this case, we get

$$\chi_{abc} \approx \frac{e^2 \overline{\Delta}_a}{2\hbar^2} \frac{1}{\omega_\Sigma + i\Gamma} \sum_{\mathbf{p}} \left(\frac{\mathcal{A}^{vc}_b \mathcal{A}^{cv}_c}{\omega_1 + i\gamma - \omega_{vc}} + \frac{\mathcal{A}^{cv}_b \mathcal{A}^{vc}_c}{\omega_1 + i\gamma - \omega_{cv}} + \frac{\mathcal{A}^{vc}_b \mathcal{A}^{cv}_c}{\omega_2 + i\gamma - \omega_{cv}} + \frac{\mathcal{A}^{cv}_b \mathcal{A}^{vc}_c}{\omega_2 + i\gamma - \omega_{vc}} \right). \tag{S115}$$

Under the same assumptions, the linear electric susceptibility (which determines the polarization [15]) is given by

$$\chi^{(1)}_{ab}(\omega) \approx -\frac{e^2}{\hbar\epsilon_0} \sum_{\mathbf{p}} \left(\frac{\mathcal{A}^{vc}_a \mathcal{A}^{cv}_b}{\omega + i\gamma - \omega_{cv}} - \frac{\mathcal{A}^{cv}_a \mathcal{A}^{vc}_b}{\omega + i\gamma - \omega_{vc}} \right). \tag{S116}$$

We consider a linearly polarized input, $c = b$, and take the clean limit for the total-frequency damping, $\Gamma \to 0$, in which case the Raman susceptibility becomes

$$\chi_{abb} \approx \frac{e^2 \overline{\Delta}_a}{2\hbar^2} \frac{1}{\omega_\Sigma} \sum_{\mathbf{p}} \left(\frac{2\bar{\omega}_1 \mathcal{A}^{vc}_b \mathcal{A}^{cv}_b}{\bar{\omega}_1^2 - \omega_{cv}^2} + \frac{2\bar{\omega}_2 \mathcal{A}^{vc}_b \mathcal{A}^{cv}_b}{\bar{\omega}_2^2 - \omega_{cv}^2} \right), \qquad \chi^{(1)}_{bb}(\omega) \approx -\frac{e^2}{\hbar\epsilon_0} \sum_{\mathbf{p}} \left(\frac{2\omega_{cv} \mathcal{A}^{vc}_b \mathcal{A}^{cv}_b}{\bar{\omega}^2 - \omega_{cv}^2} \right), \tag{S117}$$

also writing the diagonal elements of the linear susceptibility, and where $\bar{\omega}_j = \omega_j + i\gamma$. From here, we can see a correspondence between the terms in the integrands of the Raman and linear susceptibilities. Neglecting the imaginary $i\gamma$ part of ω_i when appearing in the numerator, and setting $\omega_1 = \omega$ and $\omega_2 = \omega_\Sigma - \omega$, we obtain

$$\chi_{abb}(\omega, \omega_\Sigma - \omega) \approx -\frac{\epsilon_0 \overline{\Delta}_a}{2\hbar\omega_\Sigma} \sum_{\mathbf{p}} \frac{1}{\omega_{cv}} \Big[\omega \chi^{(1)}_{bb}(\omega, \mathbf{p}) + (\omega_\Sigma - \omega) \chi^{(1)}_{bb}(\omega_\Sigma - \omega, \mathbf{p}) \Big]. \tag{S118}$$

Expanding the second term in small ω_Σ at fixed ω and retaining terms up to $O(\omega_\Sigma^0)$ gives

$$\chi_{abb}(\omega, \omega_\Sigma - \omega) \approx \frac{\epsilon_0 \overline{\Delta}_a}{2\hbar} \sum_{\mathbf{p}} \frac{1}{\omega_{cv}} \left[\frac{2\omega \operatorname{Im} \chi^{(1)}_{bb}(\omega, \mathbf{p})}{i\omega_\Sigma} - \partial_\omega [\omega \chi^{(1)*}_{bb}(\omega, \mathbf{p})] \right] + O(\omega_\Sigma), \tag{S119}$$

noting that $\chi^{(1)}_{bb}(-\omega, \mathbf{p}) = \chi^{(1)*}_{bb}(\omega, \mathbf{p})$. Writing the dielectric tensor as $\epsilon_{ab}(\omega) = \epsilon_0[\delta_{ab} + \chi^{(1)}_{ab}(\omega)]$, and for a system with approximately momentum-independent gap $\hbar\omega_{cv}(\mathbf{p}) \approx \varepsilon_g$, performing the momentum sum yields Eq. (19) of the main text:

$$\chi_{abb}(\omega) \approx \frac{\overline{\Delta}_a}{\varepsilon_g} \left[\frac{\omega \operatorname{Im} \epsilon_{bb}(\omega)}{i\omega_\Sigma} - \frac{1}{2} \partial_\omega \big\{ \omega(\epsilon^*_{bb}(\omega) - \epsilon_0) \big\} \right]. \tag{S120}$$

The nonsingular term separates into

$$\partial_\omega\big[\omega(\epsilon^*_{bb}(\omega)-\epsilon_0)\big] = -i\partial_\omega\big[\omega\,\mathrm{Im}\,\epsilon_{bb}(\omega)\big]+\omega\partial_\omega\,\mathrm{Re}\,\epsilon_{bb}(\omega)+\mathrm{Re}\,\epsilon_{bb}(\omega)-\epsilon_0. \tag{S121}$$

The imaginary part gives the regular injection correction, while the real part gives the total off-resonant response.

The result contains the absorptive injection pole and the dispersive dielectric derivative appearing in the second line of Eq. (9) of Ref. [14]. Near resonance, $\hbar\omega \simeq \varepsilon_g$, the factor $\overline{\Delta}_a\omega/\varepsilon_g$ approaches $\overline{\Delta}_a/\hbar$, with the relative signs and numerical coefficients retained as written above. The full expression also includes the regular injection correction and the contribution $\mathrm{Re}\,\epsilon_{bb}(\omega)-\epsilon_0$. Neglecting these additional terms recovers the conventional form after matching coupling and normalization conventions. Throughout, we take the clean limit at fixed nonzero ω_Σ before expanding in the output frequency.

SUPPLEMENTARY NOTE 9: SYMMETRY CONSTRAINTS ON RAMAN FORCES IN THE BILAYER HALDANE MODEL

At finite Haldane gap, the equilibrium bilayer model retains threefold rotational symmetry, C_3, while mirror covariance relates opposite Haldane gaps through $M_x : (x,\delta_\mathrm{H}) \to (-x,-\delta_\mathrm{H})$. We parameterize the Haldane gap as $\delta_\mathrm{H} \propto \sin\phi_\mathrm{H}$, where the dimensionless hopping phase ϕ_H is proportional to the magnetic flux $\Phi_\triangle = \int_\triangle \mathbf{B}(\mathbf{r})\cdot d\mathbf{a}$ through a triangular plaquette. The fictitious magnetic field $\mathbf{B}(\mathbf{r})$ has zero net flux per unit cell. Like $\mathbf{B}$, the gap δ_H is an axial quantity and thus it is odd under x-reflection,

$$M_x\delta_\mathrm{H} = -\delta_\mathrm{H}. \tag{S122}$$

In other words, the positive and negative δ_H stand for two opposite chiral counterparts which map to each other under M_x reflection. Operating the time-reversal symmetry following Table II of the main text implies that displacive injection susceptibility $\alpha^{\mathrm{inj}}_{abc}$ and impulsive shift susceptibility $\beta^{\mathrm{shi}}_{abc}$ are even and odd under $\delta_\mathrm{H}\to-\delta_\mathrm{H}$, respectively:

$$\alpha^{\mathrm{inj}}_{abc}(-\delta_\mathrm{H}) = \alpha^{\mathrm{inj}}_{abc}(\delta_\mathrm{H}), \qquad \beta^{\mathrm{shi}}_{abc}(-\delta_\mathrm{H}) = -\beta^{\mathrm{shi}}_{abc}(\delta_\mathrm{H}). \tag{S123}$$

Note that the frequency dependence of the Raman responses are assumed implicit for the sake of shorthand notation. The regular injection correction, $\beta^{\text{reg-inj}} = (i/2)\partial_\omega\alpha^{\mathrm{inj}}$, inherits the parity of α^{inj} under $\delta_\mathrm{H}\to-\delta_\mathrm{H}$. The off-resonant contributions are outside the scope of the following symmetry analysis.

A. M_x: mirror covariance

The injection and shift contributions to the Raman force read

$$\mathcal{F}_a = \mathcal{F}^{\mathrm{inj}}_a + \mathcal{F}^{\mathrm{shi}}_a = \sum_{bc}\left[\frac{\alpha^{\mathrm{inj}}_{abc}(\delta_\mathrm{H})}{i\omega_\Sigma}+\beta^{\mathrm{shi}}_{abc}(\delta_\mathrm{H})\right]E_bE_c. \tag{S124}$$

Frequency arguments and the frequency integral (Eq. (2) of the main text) are suppressed for brevity. Applying the x-reflection, M_x, we obtain

$$(M_x\boldsymbol{\mathcal{F}})_a = \sum_{bc}\left\{\frac{[M_x\cdot\boldsymbol{\alpha}^{\mathrm{inj}}(\delta_\mathrm{H}) : M_x^{-1}M_x^{-1}]_{abc}}{i\omega_\Sigma}+[M_x\cdot\boldsymbol{\beta}^{\mathrm{shi}}(\delta_\mathrm{H}) : M_x^{-1}M_x^{-1}]_{abc}\right\}(M_x\mathbf{E})_b(M_x\mathbf{E})_c \tag{S125}$$

where

$$M_x\boldsymbol{\mathcal{F}} = \begin{bmatrix}-\mathcal{F}_x\\ \mathcal{F}_y\end{bmatrix}, \qquad M_x\mathbf{E} = \begin{bmatrix}-E_x\\ E_y\end{bmatrix} \tag{S126}$$

Here we should note that, although the Raman force and electric field vectors transform similarly under the mirror operation M_x, they do not transform in the same way under inversion, which also sends $y\to-y$ and $z\to-z$. The Raman force remains invariant under inversion, since $z\to-z$ exchanges the two layers, whereas the electric field is an ordinary vector and is odd under inversion. Moreover, the mirror covariance implies that

$$[M_x\cdot\boldsymbol{\alpha}^{\mathrm{inj}}(\delta_\mathrm{H}) : M_x^{-1}M_x^{-1}]_{abc} = \alpha^{\mathrm{inj}}_{abc}(M_x\delta_\mathrm{H}) = \alpha^{\mathrm{inj}}_{abc}(-\delta_\mathrm{H}) = \alpha^{\mathrm{inj}}_{abc}(\delta_\mathrm{H}), \tag{S127}$$

$$[M_x\cdot\boldsymbol{\beta}^{\mathrm{shi}}(\delta_\mathrm{H}) : M_x^{-1}M_x^{-1}]_{abc} = \beta^{\mathrm{shi}}_{abc}(M_x\delta_\mathrm{H}) = \beta^{\mathrm{shi}}_{abc}(-\delta_\mathrm{H}) = -\beta^{\mathrm{shi}}_{abc}(\delta_\mathrm{H}). \tag{S128}$$

Considering the above symmetry argument, Eq. (S125) can be written for each component:

$$-\mathcal{F}_x = \left(\frac{\alpha^{\rm inj}_{xxx}}{i\omega_\Sigma} - \beta^{\rm shi}_{xxx}\right) E_x E_x + \left(\frac{\alpha^{\rm inj}_{xyy}}{i\omega_\Sigma} - \beta^{\rm shi}_{xyy}\right) E_y E_y - \left(\frac{\alpha^{\rm inj}_{xxy}}{i\omega_\Sigma} - \beta^{\rm shi}_{xxy}\right) E_x E_y - \left(\frac{\alpha^{\rm inj}_{xyx}}{i\omega_\Sigma} - \beta^{\rm shi}_{xyx}\right) E_y E_x \tag{S129}$$

$$\mathcal{F}_y = \left(\frac{\alpha^{\rm inj}_{yyy}}{i\omega_\Sigma} - \beta^{\rm shi}_{yyy}\right) E_y E_y + \left(\frac{\alpha^{\rm inj}_{yxx}}{i\omega_\Sigma} - \beta^{\rm shi}_{yxx}\right) E_x E_x - \left(\frac{\alpha^{\rm inj}_{yyx}}{i\omega_\Sigma} - \beta^{\rm shi}_{yyx}\right) E_y E_x - \left(\frac{\alpha^{\rm inj}_{yxy}}{i\omega_\Sigma} - \beta^{\rm shi}_{yxy}\right) E_x E_y. \tag{S130}$$

Equating expressions for each of $\mathcal{F}_x$ and $\mathcal{F}_y$ before and after M_x reflection, we obtain

$$\alpha^{\rm inj}_{xxx} = \alpha^{\rm inj}_{xyy} = \alpha^{\rm inj}_{yyx} = \alpha^{\rm inj}_{yxy} = 0; \qquad \beta^{\rm shi}_{yyy} = \beta^{\rm shi}_{yxx} = \beta^{\rm shi}_{xxy} = \beta^{\rm shi}_{xyx} = 0, \tag{S131}$$

with remaining elements surviving.

B. C_3: rotational symmetry

Moving onto three-fold rotation, we consider components of $\alpha^{\rm inj}_{abc}$ and $\beta^{\rm shi}_{abc}$ separately. The former of these, considering the results from above, gives force components of

$$\mathcal{F}^{\rm inj}_x = \frac{1}{i\omega_\Sigma}\left\{\alpha^{\rm inj}_{xxy} E_x E_y + \alpha^{\rm inj}_{xyx} E_y E_x\right\} \tag{S132}$$

$$\mathcal{F}^{\rm inj}_y = \frac{1}{i\omega_\Sigma}\left\{\alpha^{\rm inj}_{yyy} E_y E_y + \alpha^{\rm inj}_{yxx} E_x E_x\right\}. \tag{S133}$$

Acting once with the C_3 operator, vectors transform as

$$C_3\begin{bmatrix}\hat{x}\\ \hat{y}\end{bmatrix} = \begin{bmatrix}-\frac{1}{2}\hat{x} + \frac{\sqrt{3}}{2}\hat{y}\\ -\frac{\sqrt{3}}{2}\hat{x} - \frac{1}{2}\hat{y}\end{bmatrix}, \quad C_3\begin{bmatrix}\mathcal{F}_x\\ \mathcal{F}_y\end{bmatrix} = \begin{bmatrix}-\frac{1}{2}\mathcal{F}_x + \frac{\sqrt{3}}{2}\mathcal{F}_y\\ -\frac{\sqrt{3}}{2}\mathcal{F}_x - \frac{1}{2}\mathcal{F}_y\end{bmatrix}, \quad C_3\begin{bmatrix}E_x\\ E_y\end{bmatrix} = \begin{bmatrix}-\frac{1}{2}E_x + \frac{\sqrt{3}}{2}E_y\\ -\frac{\sqrt{3}}{2}E_x - \frac{1}{2}E_y\end{bmatrix}, \tag{S134}$$

and pseudovectors transform as regular vectors, as rotation is a proper symmetry operation, meaning $\delta_{\rm H}$ is invariant under C_3. Moreover, the Raman-force susceptibility tensors are invariant due to the three-fold rotational symmetry:

$$[C_3 \cdot \boldsymbol{\alpha}^{\rm inj}(\delta_{\rm H}) : C_3^{-1} C_3^{-1}]_{abc} = \alpha^{\rm inj}_{abc}(\delta_{\rm H}), \tag{S135}$$

$$[C_3 \cdot \boldsymbol{\beta}^{\rm shi}(\delta_{\rm H}) : C_3^{-1} C_3^{-1}]_{abc} = \beta^{\rm shi}_{abc}(\delta_{\rm H}). \tag{S136}$$

Looking just at $\mathcal{F}^{\rm inj}_y$, rotation yields

$$-\frac{\sqrt{3}}{2}\mathcal{F}^{\rm inj}_x - \frac{1}{2}\mathcal{F}^{\rm inj}_y = \frac{3\alpha^{\rm inj}_{yyy} + \alpha^{\rm inj}_{yxx}}{4(i\omega_\Sigma)} E_x E_x + \frac{\sqrt{3}(\alpha^{\rm inj}_{yyy} - \alpha^{\rm inj}_{yxx})}{4(i\omega_\Sigma)} E_x E_y + \frac{\sqrt{3}(\alpha^{\rm inj}_{yyy} - \alpha^{\rm inj}_{yxx})}{4(i\omega_\Sigma)} E_y E_x + \frac{\alpha^{\rm inj}_{yyy} + 3\alpha^{\rm inj}_{yxx}}{4(i\omega_\Sigma)} E_y E_y. \tag{S137}$$

Substituting in $\mathcal{F}^{\rm inj}_x$ and $\mathcal{F}^{\rm inj}_y$ from Eqs. (S132) and (S133), and equating terms with the same $E^b E^c$, we obtain simultaneous equations with solutions

$$-\alpha^{\rm inj}_{yyy} = \alpha^{\rm inj}_{yxx} = \alpha^{\rm inj}_{xxy} = \alpha^{\rm inj}_{xyx} \neq 0. \tag{S138}$$

Looking at $\beta^{\rm shi}_{abc}$ now, our remaining terms give forces of

$$\mathcal{F}^{\rm shi}_x = \beta^{\rm shi}_{xxx} E_x E_x + \beta^{\rm shi}_{xyy} E_y E_y \tag{S139}$$

$$\mathcal{F}^{\rm shi}_y = \beta^{\rm shi}_{yxy} E_x E_y + \beta^{\rm shi}_{yyx} E_y E_x. \tag{S140}$$

Acting the $\mathcal{C}_3$ operator on $\mathcal{F}^{\rm shi}_x$, we obtain

$$-\frac{1}{2}\mathcal{F}^{\rm shi}_x + \frac{\sqrt{3}}{2}\mathcal{F}^{\rm shi}_y = \frac{\beta^{\rm shi}_{xxx} + 3\beta^{\rm shi}_{xyy}}{4} E_x E_x - \frac{\sqrt{3}(\beta^{\rm shi}_{xxx} - \beta^{\rm shi}_{xyy})}{4} E_x E_y - \frac{\sqrt{3}(\beta^{\rm shi}_{xxx} - \beta^{\rm shi}_{xyy})}{4} E_y E_x + \frac{3\beta^{\rm shi}_{xxx} + \beta^{\rm shi}_{xyy}}{4} E_y E_y. \tag{S141}$$

Substituting in $\mathcal{F}_x^{\rm shi}$ and $\mathcal{F}_y^{\rm shi}$ from Eqs. (S139) and (S140), then solving the resulting simultaneous equations, we obtain

$$-\beta_{xxx}^{\rm shi} = \beta_{xyy}^{\rm shi} = \beta_{yxy}^{\rm shi} = \beta_{yyx}^{\rm shi} \neq 0. \tag{S142}$$

The final symmetry results, summarized in Eqs. (S138) and (S142) and identifying the non-vanishing tensor elements of the injection and shift responses, are collected in Eq. (21) of the main text and are in exact agreement with our analytical and numerical calculations.

SUPPLEMENTARY NOTE 10: TEMPERATURE DEPENDENCE OF LINEARLY-POLARIZED RAMAN FORCES

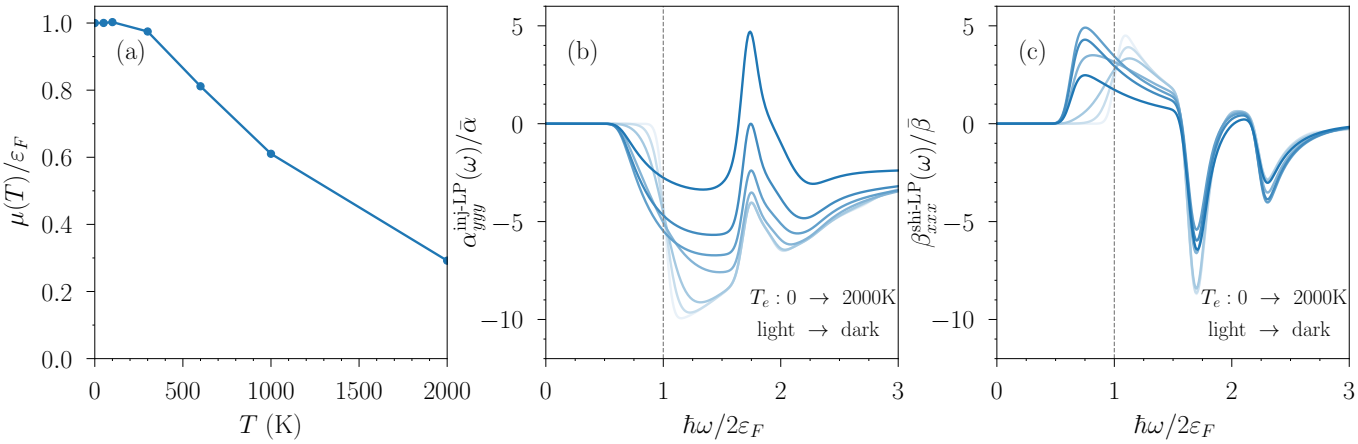
Here, we briefly provide and discuss the numerical results for the resonant Raman shear force susceptibilities due to LP light at various temperatures. We first compute the chemical potential at different temperatures and then obtain the numerical result for the Raman-force susceptibilities. The chemical potential is obtained by numerically solving $n = n_e(T) - n_h(T) = n_e(0) - n_h(0)$ for μ, where $n_{e(h)}(T)$ is the density of electrons (holes) at temperature, T. We calculate the differences in density using

$$n = n_e(T) - n_h(T) = \int_{\rm BZ} \frac{d^2\mathbf{p}}{(2\pi)^2} \left\{ \sum_{m\in\text{conduction}} f_m - \sum_{m\in\text{valence}} (1 - f_m) \right\} = \int_{\rm BZ} \frac{d^2\mathbf{p}}{(2\pi)^2} \left\{ \sum_{m\in\text{all bands}} f_m - N_{\rm val} \right\}, \tag{S143}$$

where $N_{\rm val} = 2$ is the number of valence bands, zero-temperature chemical potential is the Fermi energy $\mu(0) = \varepsilon_F$ which is set by the carrier density n, and Fermi distribution function of band m reads

$$f_m = \frac{1}{1 + \exp\left\{ \frac{\varepsilon_m(\mathbf{p}) - \mu(T)}{k_B T} \right\}}. \tag{S144}$$

By solving Eq. (S143), for a given Fermi energy ε_F we obtain the chemical potential at different temperature. The dotted points in Supplementary Fig. 3a indicate the values of chemical potential we calculated at various temperatures. As seen it stays nearly constant until the temperature exceeds 100 K, when it starts to decrease quickly, with this descent slowing down as one increases temperature further. We use the chemical potential values shown in panel (a) and the finite-temperature Fermi distribution, Eq. (S144), to compute the injection and shift Raman-force responses at various temperatures, shown in panels (b) and (c), respectively.



Supplementary Fig. 3. (a) Chemical potential, μ as a function of temperature, T in the bilayer Haldane model relative to the Fermi energy, $\epsilon_F = 0.1$ eV. (b, c) Spectra for LP (b) injection (c) shift shear Raman-force susceptibility at different electronic temperatures with $\phi = \pi/80$ and $\delta = 0$, where we account for both population spreading and changing of chemical potential due to increasing temperature. Note that $\bar{\alpha} = 100\,\text{nN}/(\text{V}^2\,\text{ps})$ and $\bar{\beta} = \text{nN}/\text{V}^2$. The same units and parameter values are used for the LP Raman-force responses presented in Fig. 4 of the main text. From light to dark, the curves correspond to $T = 0$, 50, 100, 300, 600, 1000, and 2000 K.

Beyond simple thermal broadening, raising the electron temperature depletes carriers in the UVB and populates the LCB. This redistribution is partly compensated by the downward shift of the chemical potential with increasing temperature. Together, these effects in the electronic distribution account for most of the temperature dependence observed in the response functions. At low temperature, the absorption edge at $2\epsilon_F$, arising from UVB–LCB transitions, gradually flattens and, above 300K, shifts entirely to lower energies. This behaviour is driven by the reduced LCB occupation near the Dirac point, caused both by thermal spreading to higher energies and by the lowering of the chemical potential. As a result, transitions near the band (Haldane) gap become increasingly allowed and are no longer Pauli blocked.

Remarkably, the increased LCB population enhances LCB–UCB transitions, which appear as a sharp peak opposite in sign to the absorption step in the injection response. In contrast, the corresponding contribution to the shift response is reduced, since this response is maximal near the Dirac point and the thermally broadened LCB population shifts resonances away from it. Interestingly, beyond 600K the shift-response peak grows again, due to the competition between (i) the detrimental effect of population spreading in the LCB and (ii) the lowering chemical potential, which creates additional vacancies in the UVB and enables previously forbidden LVB–UVB transitions.

[1] G. Baym and L. P. Kadanoff, Phys. Rev. **124**, 287 (1961).
[2] L. P. Kadanoff and G. Baym, *Quantum Statistical Mechanics* (W. A. Benjamin, Inc., 1962).
[3] H. Rostami and E. Cappelluti, npj 2D Materials and Applications **5**, 50 (2021).
[4] G. D. Mahan, *Many Particle Physics* (Kluwer Academic/Plenum Publishers, 2000).
[5] T. Holder, D. Kaplan, and B. Yan, Phys. Rev. Res. **2**, 033100 (2020).
[6] H. Rostami, Phys. Rev. B **106**, 155405 (2022).
[7] J. Ahn, G.-Y. Guo, and N. Nagaosa, Phys. Rev. X **10**, 041041 (2020).
[8] H. Watanabe and Y. Yanase, Phys. Rev. X **11**, 011001 (2021).
[9] G. B. Ventura, D. J. Passos, J. M. B. Lopes dos Santos, J. M. Viana Parente Lopes, and N. M. R. Peres, Phys. Rev. B **96**, 035431 (2017).
[10] D. E. Parker, T. Morimoto, J. Orenstein, and J. E. Moore, Phys. Rev. B **99**, 045121 (2019).
[11] A. Gao, Y.-F. Liu, J.-X. Qiu, B. Ghosh, T. V. Trevisan, Y. Onishi, C. Hu, T. Qian, H.-J. Tien, S.-W. Chen, M. Huang, D. Bérubé, H. Li, C. Tzschaschel, T. Dinh, Z. Sun, S.-C. Ho, S.-W. Lien, B. Singh, K. Watanabe, T. Taniguchi, D. C. Bell, H. Lin, T.-R. Chang, C. R. Du, A. Bansil, L. Fu, N. Ni, P. P. Orth, Q. Ma, and S.-Y. Xu, Science **381**, 181 (2023).
[12] H. Rostami and M. Polini, Phys. Rev. B **97**, 195151 (2018).
[13] E. I. Blount, *Solid State Physics: Advances in Research and Applications*, edited by F. Seitz and D. Turnbull (Elsevier, Amsterdam, 1962).
[14] T. E. Stevens, J. Kuhl, and R. Merlin, Phys. Rev. B **65**, 144304 (2002).
[15] J. E. Sipe and A. I. Shkrebtii, Phys. Rev. B **61**, 5337 (2000).